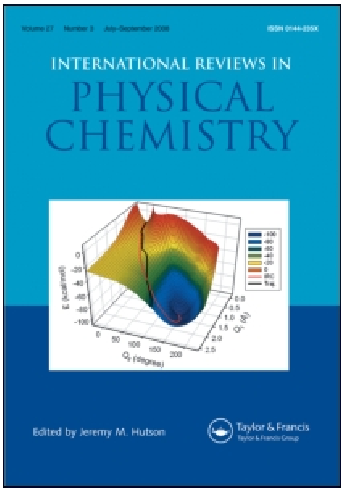

International Reviews in Physical Chemistry
Publication details, including instructions for authors and subscription information:
http://www.informaworld.com/smpp/title~content=t713724383

Study of Adsorbed Molecules by Electron Energy Loss Spectroscopy

C. N. R. Rao[a]; A. Srinivasan[a]; K. Jagannathan[a]
[a] Solid State and Structural Chemistry Unit, Indian Institute of Science, Bangalore, India

To cite this Article Rao, C. N. R. , Srinivasan, A. and Jagannathan, K.(1981) 'Study of Adsorbed Molecules by Electron Energy Loss Spectroscopy', International Reviews in Physical Chemistry, 1: 1, 45 — 91
To link to this Article: DOI: 10.1080/01442358109353242
URL: http://dx.doi.org/10.1080/01442358109353242

International Reviews in Physical Chemistry (1981), *1* (45–91)
© 1981 Butterworths

STUDY OF ADSORBED MOLECULES BY ELECTRON ENERGY LOSS SPECTROSCOPY*

C. N. R. RAO,† A. SRINIVASAN AND K. JAGANNATHAN

Solid State and Structural Chemistry Unit, Indian Institute of Science, Bangalore—560012, India

ABSTRACT

Electron energy loss spectroscopy (EELS) has become a very important tool in the study of the surface chemistry of solids. Besides providing information on the vibrational spectra of adsorbed molecules, EELS (with primary electrons of low energy, $\leqslant 5$ eV) also throws light on metal-ligand vibrations. The vibrational spectra from EELS are useful in understanding gas-solid interactions and the nature of the molecular species such as the state of hybridization of orbitals in hydrocarbon fragments bound to the surface. By employing primary electrons of higher energies (30–300 eV), electronic excitations of adsorbed molecules as well as the adsorbents themselves can be fruitfully studied. This article describes the up-to-date status of EELS in the study of adsorbed molecules and surveys all the important literature data and correlations.

INTRODUCTION

Electron energy loss spectroscopy (EELS) is one of the powerful techniques of modern electron spectroscopy well suited for the study of vibrational and electronic excitations in molecules. High resolution electron energy loss spectroscopy employing low-energy primary electron beams gives valuable information pertaining to vibrational spectra in molecules and usefully complements the information obtained from infrared and Raman spectroscopy. By employing higher energy primary electron beams information is obtained on electronic transitions in molecules. Studies of free molecules employing EELS have been reviewed extensively (Trajmar, Rice and Kupperman, 1970; Kuppermann, Flicker and Mosher, 1979; Rao *et al.*, 1980). However, apart from earlier, more general surveys (Thomas, 1974; Ertl and Küppers, 1974; Sheppard and Nguyen, 1978) there has been no comprehensive review of the vibrational spectra and electronic excitations of adsorbed molecules, investigated through energy loss spectroscopy. For adsorbed molecules, vibrational frequencies from EELS can be effectively used along with the data from studies employing other techniques like infrared spectroscopy, Auger spectroscopy and photoelectron spectroscopy to understand the nature of bonding of the molecules to the surface and also the stereochemistry of the adsorbate-adsorbent system. Information on electronic excitations obtained from EELS is useful to understand the electronic levels of both the adsorbed molecules and the surface; the effect of adsorbed molecules on the surface state and interband transitions as well as on the surface plasmon and bulk plasmon transitions of solids is also fruitfully studied. In view of the increasing importance of these studies in understanding heterogeneous catalysis as well as other

---

* Communication No. 101 from Solid State and Structural Chemistry Unit.
† To whom all correspondence should be addressed.

aspects of adsorbate-adsorbent (gas-solid) interactions, we review results from EELS studies of adsorbed molecules in this article. We present the more important findings and correlations in the text and summarize much of the experimental data in tabular form along with all the important references to the recent literature. It should be possible readily to obtain all the other literature references through those cited in the article. In line with current practice we have employed reciprocal centimeter units (cm^{-1}) while discussing vibrational spectra and electron volts while discussing electronic transitions.

BASIC FACTS ABOUT ENERGY LOSS SPECTROSCOPY

In electron energy loss spectroscopy, a monochromatic beam of electrons interacts with molecules or a solid under investigation. One then measures the energy of the electrons that are inelastically scattered or reflected. The loss in energy of electrons thus measured contains information on the kind of excitation process undergone by the system investigated. The technique is somewhat similar to Raman spectroscopy where the energy of the scattered radiation is measured.

An electron spectrometer consists of an electron gun, a monochromator, a target chamber and an energy analyser, all built nowadays into a bakeable stainless steel chamber in which ultra-high vacuum can be achieved. The apparatus is usually magnetically shielded by Mu metal to reduce the residual magnetic fields to a negligible level. Electrons emitted from a hot Th-W cathode are focused and monochromatized and after reflection from the surface are energy analysed. Typically, two spherical mirror analysers are used for the monochromator and the analyser. Energy loss measurements are performed with a constant energy window by sweeping the retarding voltage between the target and the analyser chambers so that the path energy of the electrons in the analyser is kept constant. The data are usually obtained in the second derivative mode.

Information on vibrational spectra of adsorbed molecules obtained by EELS is similar to reflection absorption infrared spectroscopy, EELS having, by one or two orders of magnitude, a greater sensitivity. Furthermore, in EELS we have a wider range of accessible energies compared to infrared spectroscopy. Thus, in infrared studies of adsorbed molecules we cannot readily proceed below 600 cm^{-1} while EELS provides information even on metal-ligand stretching vibrations (for example, M–C stretching vibration in the case of CO adsorbed on metals occurring well below 400 cm^{-1}). The main disadvantage of EELS is its poor resolution. In high resolution EELS, 8–10 meV (60–80 cm^{-1}) may be achieved, and the uncertainty in absolute measurements is around ± 5 cm^{-1}. Another limitation of EELS is that it can be studied only under good vacuum; this would mean that studies of surfaces under realistic *in vivo* conditions (e.g., heterogeneous catalysts) cannot be carried out. On the other hand, the technique possesses remarkable sensitivity. In high resolution EELS even a fraction of a monolayer can be detected. For example, in the case of CO adsorbed on metals, less than 0.02 monolayer can be detected (Demuth and Ibach, 1979b). Although normally intensities in EELS are not used widely, quantitative comparisons of intensities can be made by evaluating effective ionic charges of adsorption systems if the electron acceptance angle in the spectrometer is known precisely (Ibach, 1977).

EELS as well as absorption of infrared radiation are caused by the dipole moment change of the surface vibration and the same selection rules apply in both these techniques. A comparison of absolute intensities between the techniques is possible Ibach (1977) has discussed photon-dipole and electron-dipole interactions. Theoretical relations between cross sections and dipole moments of the adsorbate vibrations are available for both these scattering processes. Vibrational spectra of adsorbed molecules as studied by infrared spectroscopy or EELS are governed by only vibrations which give rise to dipole moments perpendicular to the surface. Dipoles parallel or perpendicular to the surface of a metal produce virtual image dipoles. A bond stretching vibration which gives a dipole change parallel to the surface will produce an equal and opposite change in the induced image dipole in the metal substrate. The net dipole change is therefore zero in the case of such a vibration. An oscillating dipole perpendicular to the surface is reinforced by the oscillating image dipole. These surface normal dipole selection rules have been discussed by Pearce and Sheppard (1976) and also by Backx *et al.* (1977b).

The mechanism of diffused scattering of electrons by dipole-forbidden transitions has been studied by Thomas and Weinberg (1979b) who have compared the calculated scattering probabilities with the measurements on the so-called β_1 phase of hydrogen (at high coverages) on W(100) to illustrate the magnitude of this effect in terms of dipole and quadrupole derivatives. Dipole-forbidden transitions are expected to be two to three orders of magnitude weaker than dipole scattering in the specular direction. Dipole-forbidden transitions could, however, make a significant contribution in the off-specular direction. MSXα calculations on electron scattering cross sections for adsorbed hydrogen (as well as N_2 and CO) have been carried out by Davenport, Ho and Schrieffer (1978). These calculations show how the characteristics of inelastic cross sections (as functions of direction and exciting energy of electrons) can be utilized to study adsorbed molecules. Inelastic scattering of slow electrons from molecules adsorbed on a metal surface has been studied by Pearson (1980). Previous calculations have been improved by including coulomb interaction between the incident electrons and the induced charge density that they give rise to in the surface region of the metal.

VIBRATIONAL SPECTRA

We shall discuss vibrational frequencies of adsorbed molecules obtained from high resolution EELS by proceeding from adsorbate to adsorbate. This constitutes a comparative study of the behaviour of a variety of simple molecules with respect to different adsorbent surfaces.

Hydrogen

Chemisorption of hydrogen on Si, Pt or W is dissociative and the surface vibrational modes obtained from EELS are summarized in *Table 1.* In the case of Si, only one stretching frequency of 2071 cm^{-1} has been reported by Froitzheim, Ibach and Lehwald (1975). In the case of Pt, both symmetric (A_1 mode) and asymmetric (E mode) stretching vibration frequencies (at 550 and 1270 cm^{-1} respectively) due to atomic hydrogen adsorbed on a three-fold hollow site have been identified by Baro, Ibach and Bruchmann (1979). Baro and Ibach (1980) have more recently confirmed these two frequencies and have in addition assigned a loss peak at 1130 cm^{-1} to a bridge site hydrogen.

Adsorption of atomic hydrogen on W has been investigated in great detail by Backx *et al.* (1977a), Ho, Willis and Plummer (1978), Barnes and Willis (1978), Willis (1979), Willis, Ho and Plummer (1979). Vibrational force constants of hydrogen adsorbed on W are found to be independent of surface geometrical environment (Backx *et al.*, 1977a). Angle-dependent measurements of Ho, Willis and Plummer (1978) and Willis, Ho and Plummer (1979) at a saturation coverage of chemisorbed hydrogen on W(100) show a single energy loss at 1048 cm^{-1} in the specular direction. This loss peak can be assigned to the symmetric stretching of a bridge hydrogen; in the off-specular direction additional losses are seen at 645, 1290 and 2096 cm^{-1} of which the first two seem to be due to the

TABLE 1. Vibrational spectra of hydrogen adsorbed on metals

Surface	Ep (eV)	Temperature (K)	Coverage*	Energy loss peaks (cm^{-1})				Remarks	Reference
Si(111)	5	300	400 L	2071					Froitzheim, Ibach and Lehwald, 1975
Pt(111)	5	90	>10 L		1230		550		Baro, Ibach and Bruchmann, 1979
			<2 L	additional loss at 860					
Pt[6(111) × ($\bar{1}$11)]	5	90	All coverages	1270		1130[a]	550[a]		Baro and Ibach, 1980
W(111)	5	300	20 L	1290[b]					Backx *et al.*, 1977a
W(110)	4	300	10 L	1265[b]		766			
W(100)	5	300	$\theta = 2$	1249[b]		1048			
W(100)	9.7	300	θ_{sat}			1048		Specular direction	Willis, Ho and Plummer, 1979
			θ_{sat}	2096	1290	1048	645	Off-specular direction	Ho, Willis and Plummer, 1978
W(100)	5.5	300	θ_{sat}	1290	1048	645		c(2 × 2) H	Barnes and Willis, 1978

[a] D_2 frequencies are 870 and 410 cm^{-1}.

[b] Jayasooriya *et al.* (1980) assign this to $\mathrm{W}\overset{\mathrm{H}}{\diagup\ \diagdown}\mathrm{W}$ with the W atoms in contact.

* 1 L (Langmuir unit of 'exposure') ≡ 1 × 10^{-6} torrs.

γMH and asymmetric νMH modes of the bridged hydrogen and the 2096 cm^{-1} peak is the overtone of the symmetric stretching mode. The vibrational frequencies show dependence on the W–H–W angle which changes due to reconstruction of the W lattice. Comparison with infrared frequencies of the transition metal hydride complexes has provided structural parameters for the W(100) c(2 × 2) H reconstructed surface (Barnes and Willis, 1978; Willis, 1979). Differential inelastic scattering cross sections of the vibrational modes indicate that adjacent W atoms are tilted out of the surface plane (Willis, 1979). A puckered ($\sqrt{2} \times \sqrt{2}$) R 45° layer model involving both vertical and parallel W atomic shifts appears to be consistent with the observed spectra. Jayasooriya *et al.* (1980) have fruitfully discussed the vibrational spectra of hydrogen chemisorbed on metal surfaces in the light of data on model cluster compounds; adsorption sites for hydrogen on low index planes of W are suggested on the basis of high resolution EELS data. Hydrogen adsorbed on a bridge site between two metal atoms appears to be present at both low coverage (β_2) and high coverage (β_1) sites in the case of W(100).

Nitrogen

On W(100), terminal as well as bridge bonded N_2 molecules have been identified by Ho, Willis and Plummer (1980) who also observe dissociated nitrogen atoms on the surface. The energy loss peak due to bridge nitrogen (~1440 cm^{-1}) shifts to higher frequency (~1760 cm^{-1}) on co-adsorption of hydrogen; this shift is attributed to displacement of nitrogen from bridge to on-top sites. Dissociative adsorption occurs at 300 K giving rise to a loss peak around 480 cm^{-1}. The various losses observed at 125 K are 480 cm^{-1} (nitrogen atom sitting at the centre of a four-fold site), 600 cm^{-1} (W–N_2 linear site), 1000 cm^{-1} (W–N of dissociated species), 1440 cm^{-1} (N–N bridge bonded to two W atoms) and 2120 cm^{-1} (N–N stretching vibration of molecularly adsorbed N_2).

Oxygen

Adsorption of oxygen on metals is generally dissociative. The important energy loss peaks found in metal-oxygen systems are presented in *Table 2*. Localized modes due to adsorbed oxygen on Si(111) surface are reported to be around 758, 1048 and 1410 cm^{-1} by Ibach *et al.* (1973) who find that the first two peaks increase linearly with oxygen exposures (up to 5×10^3 L) while the last increases non-linearly. These workers propose that oxygen is present as a 'peroxy-group' between two Si sites.

Vibrational losses due to localized modes of oxygen chemisorbed on Ni(100) in consecutive p(2 × 2) and c(2 × 2) structures are found at 427 and 314 cm^{-1} respectively by Andersson (1979a); the modes with sulphur at the corresponding coverages and surface structures are at 371 and 355 cm^{-1}. The large change in the vibrational excitation energy in the two oxygen structures is considered to be due to a low potential barrier for oxygen dissolution into the Ni substrate. An intermediate oxide layer on Ni with a characteristic loss peak of 908 cm^{-1} has been observed by Dalmai-Imelik, Bertolini and Rousseau (1977); a multiple loss spectrum with a spacing of 544 cm^{-1} is observed due to scattering by long-wavelength optical phonons of the oxide. Ibach and Bruchmann (1980) find that surface phonons of metals at certain points of the 2-dimensional Brillouin zone can be observed due to the coupling provided by commensurable adsorbate oxygen lattices. A 135 cm^{-1} loss is attributed to the Ni(111) p(2 × 2) structure; a loss peak at 265 cm^{-1} shifts to 240 cm^{-1} when p(2 × 2) shifts to ($\sqrt{3} \times \sqrt{3}$) R 30° structure at 410 K.

In the case of W(100) surface, Froitzheim, Ibach and Lehwald (1976) have found a single surface vibration (605 cm^{-1}) of dissociated oxygen atoms at $\theta < 0.25$. At higher coverages, the spectrum becomes complex. On Pt(111), Gland, Sexton and Fisher (1980)

TABLE 2. Vibrational spectra of oxygen adsorbed on metals

Surface	Ep (eV)	Temperature (K)	Coverage	Energy loss peaks (cm^{-1})	Remarks	Reference
Si(111)	7	250	560–800 L	1410 1048 758		Ibach *et al.*, 1973
Ni(100)	0.9	500	2 L	427 p(2 × 2) O	Peaks for S at 371 and 355 cm^{-1}	Andersson, 1979a
			50 L	314 c(2 × 2) O		
Ni(100)	4	500–800	>0.2 L	908 hexagonal LEED pattern peaks at every 544 cm^{-1}	NiO(100) on Ni(100)	Dalmai-Imelik, Bertolini and Rousseau, 1977
		700–900	3 L			
Ni(111)	2	275	2.8 L	580 265 135 p(2 × 2)		Ibach and Bruchmann, 1980
		215	10 L	580 240 ($\sqrt{3} \times \sqrt{3}$) R 30°		
Cu(100)	5	470	50 L	330		Sexton, 1979b
			1500 L	290 ($\sqrt{2} \times 2\sqrt{2}$) R 45°		
Cu(110)				~400		Wendelken and Ulehla, 1979
Ru(001)	4	100	Low θ	516		Thomas and Weinberg, 1979a
			High θ	596 (2 × 2)		
W(100)	5	300	$\theta = 0.17$	605		Andersson, 1977b
			$\theta = 0.3$	629 403		
			$\theta = 0.5$	Additional loss peak at 725		
			$\theta = 0.85$	725 524		
			1	Only one peak at 1008		
		1200	1.5 L	991 725 564	Surface annealed after exposure	
Pt(111)	4.7	100	5 L	870 (ν o–o), 710 (possibly on defect sites) 390 (ν Pt–o)		Gland, Sexton and Fisher, 1980
	4.3	300	5 L	490 (atomic oxygen)		
	3.5	1200	120 L	760 (coupling with phonon modes of Pt oxide), 1530 (double loss)		

have recently reported molecular adsorption below 120 K, atomic oxygen in the 150–500 K temperature range and oxide formation in the range 1000–1200 K. They have assigned the peroxo structure for the molecularly adsorbed species showing a loss peak at 870 cm^{-1} along with a loss peak at 390 cm^{-1} due to Pt–O stretching. Atomic oxygen on Pt(111) gives a loss at 470 cm^{-1}.

Energy loss spectra of OH on NiO(111) recorded with different primary energies show peaks at 3707 and 7294 cm^{-1} due to OH stretching and first overtone respectively (Andersson and Davenport, 1978) these are accompanied by intrinsic NiO phonon satellites at 524 cm^{-1}. The loss intensity of the OH stretching peaks is found to be more than the dipole estimates.

Carbon monoxide

Carbon monoxide is molecularly chemisorbed on many metal surfaces at relatively low temperatures. Several investigators have studied the chemisorbed species by employing vibrational spectroscopy and this subject has been excellently reviewed by Sheppard and Nguyen (1978). A special feature in the information provided by high resolution electron energy loss spectroscopy is that related to metal-carbon stretching vibrations. A careful examination reveals that the scheme for the interpretation of C–O stretching frequencies suggested by Sheppard and Nguyen (1978) provides a sound basis for analysing the results from energy loss spectroscopy. The general scheme of Sheppard and Nguyen is as follows:

	Frequencies vary in the order
1880–1650 cm^{-1}	$B_3(111) > B_4(100) > B_5(110)$*
2000–1880 cm^{-1}	$B_2(111) > B_2(100) > B_2(110)$
2130–2000 cm^{-1}	$C_9(111) > C_8(100)$
>2130 cm^{-1}	Oxidized metal surface

(* not very certain)

Here, B refers to a bridge site and C refers to a linear site. The subscripts 2, 3, 4 etc. in the case of B sites stand for the number of atoms involved in bridging (fold) and the subscripts in the case of C sites stand for the coordination number of the metal atom. Making use of this scheme, we have summarized the available data on the chemisorption of CO on a variety of metals in *Table 3*. These data are by and large in agreement with the results obtained from infrared spectroscopic studies.

On the Ni(111) surface, the C–O stretching frequencies due to both linear and B_3 bridged species are readily assigned to loss peaks at 2050 and 1810 cm^{-1} respectively (Erley, Wagner and Ibach, 1979). On a stepped Ni[5(111) × $(\bar{1}10)$] surface, a C—O stretching frequency as low as 1520 cm^{-1} has been found by Erley *et al.* (1979) who have assigned this to a three-fold bridged CO on the step site. This low value indicates a very weak C–O bond which is probably a precursor to the decomposition of carbon monoxide. On this stepped surface, the C–O stretching frequencies for linear and B_2 sites are found in the range 2020–2060 cm^{-1} and 1900–1960 cm^{-1} respectively; the corresponding M–C (metal–carbon) stretching frequencies are at 460–480 cm^{-1} and 400–420 cm^{-1}. These workers also find a coverage dependent C–O stretching frequency in the 1900–1820 cm^{-1} range along with the corresponding M–C stretching vibration around 400 cm^{-1} which is attributed to a 2-fold and 3-fold bridge on (111) terrace as illustrated in *Fig. 1*.

TABLE 3. Vibrational spectra of carbon monoxide adsorbed on metals

Surface	Ep (eV)	Temperature (K)	Coverage	Energy loss peaks (cm^{-1})					Reference
				C–O stretching				M–C stretching	
				Linear	Bridge		Step sites and others		
Ni(111)	5	140	1.1 L			1810(B_3)		400	Erley, Wagner and Ibach, 1979
			>1.1 L	2050		1810		400	
			High θ	2050		1910		400	
Ni(111)	3	300	Low θ			1805(B_3)			Bertolini, Dalmai-Imelik and Rousseau, 1977
			High θ			1910(B_3)			
Ni[5(111) × ($\bar{1}$10)]	5	150	0.1–0.3 L	2040	1930(B_2)		1525 step 1860 site	360, 400 410, 470	Erley *et al.*, 1979
Ni(100)	1.4	173	0.3 L	2067	1942(B_2)			359, 665	Andersson, 1977a
			$\theta = 0.6$		1991(B_2)			432	
Ni(100) c(2 × 2) CO	1.4	293	<1 L	2067	1934(B_2)			480	
Ni(100) c(2 × 2) O	1.3	173	0.05 L		1959(B_2)	1749(B_4)		322	Andersson, 1977b
Ni(100) p(2 × 2) O	1.3	173	0.3 L		1934(B_2)	1749(B_4)		427	Andersson, 1977b
			10 L		1975(B_2)	1773(B_4)		371	
Cu(100)	5	100	50 L	2089				339	Sexton, 1979a
Cu(100) c(2 × 2) O	1.3	80	Low θ	2096				347	Andersson, 1979b
Cu(110)	5	80	Low θ	2080				686	Wendelken and Ulehla, 1979
		80	High θ	2096				—	
Pt(111)	5	150	0.2 L	2089				476	Hopster and Ibach, 1978
			0.4 L	2089	1854(B_2)			476, 379	
Pt(111)	5	320	2 L	2104	1878(B_2)			468, 379	Froitzheim, Ibach and Lehwald, 1977
Pt[6(111) × ($\bar{1}$11)]	5	150	0.1 L	2089		1693	1555 steps	476	Hopster and Ibach, 1978
			2 L	2104	1878(B_2)	1717	1410 and kinks	468	
W(100)	5	300	High θ	2080				363	Froitzheim, Ibach and Lehwald, 1977
W(111)	5	300	High θ		1991(B_2)			—	
W(110)	5	300	High θ		1991(B_2)			404	Backx *et al.*, 1977b
Ru(001)	4	110	0.2 L	1979				444	Thomas and Weinberg, 1979a
			5 L	2080				444	
Rh(111)	4.8	300	<0.1 L	1990				480	Dubois and Somorjai, 1980
			>0.5 L	2070	1870(B_2)			480, 420	

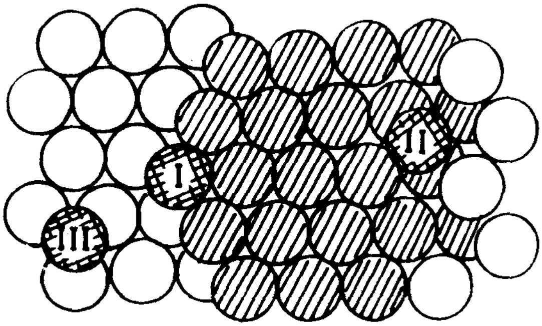

FIG. 1. Top view of a [5(111) × ($\bar{1}$10)] surface of Ni. Cross hatched circles represent CO molecules. (I) Step site; (II) 2-fold bridge close to edge; (III) 3-fold site on terrace (after Erley *et al.*, 1979).

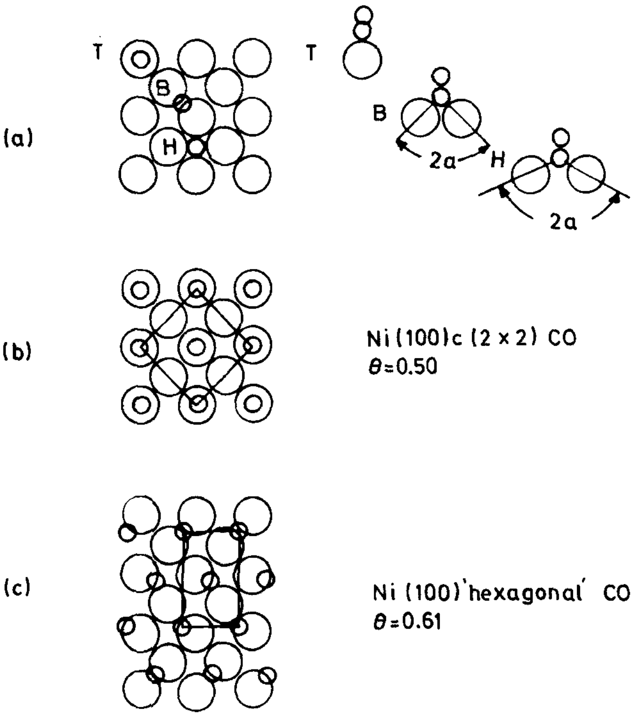

FIG. 2. (a) Models for CO bonded on Ni(100). T denotes top position (i.e. linear bond), B denotes bridge position (i.e. bridge bond) and H denotes hollow position. The $\overset{\diagup \mathrm{C} \diagdown}{\mathrm{Ni}\qquad\mathrm{Ni}}$ bond angle is denoted by 2α. (b) Model structures for the c(2 × 2) CO. (c) For the quasihexagonal ($\theta = 0.61$) CO structure. Large circles represent Ni atoms and small circles CO molecules. The particular bond configurations are inferred from vibrational loss data (after Andersson, 1977a).

Andersson (1977a and b) has reported that on the Ni(100) surface, the frequencies due to B_2 and B_4 bridged CO molecules increase with increasing coverage. Andersson (1977a) finds asymmetric and symmetric M–C stretching frequencies associated with a B_2 site at 359 and 665 cm^{-1} respectively and estimates the Ni–C stretching force constants for the bridge and linearly bonded species to be around 1.9×10^2 and 2.7×10^2 N/M respectively; the corresponding force constants for the C–O stretching mode are 14.7×10^2 and 16.3×10^2 N/M respectively. Models for CO bonded on Ni(100) surface are shown in *Fig. 2.*

Froitzheim, Ibach and Lehwald (1977) and Hopster and Ibach (1978) find additional adsorption sites on stepped Pt(111) surface compared to a smooth (111) surface (*see Fig. 3*), the latter showing C–O frequencies around 2090 and 1860 cm^{-1} due to linear and B_2 species respectively. Based on the C–O stretching frequencies, the two sites at steps are shown to be on-top of a step atom and on the terrace near the step edges. These sites are associated with low C–O frequencies (*see Table 3*) indicating a tendency of CO to dissociate.

In the case of copper only linear CO has been identified at 2096 cm^{-1} with the corresponding Cu–C stretching at 347 cm^{-1} (Sexton, 1979a; Andersson, 1979b). A slight shift in the C–O stretching frequency with coverage has been found on Cu(110) surface based on which a change from bridge to linear CO has been proposed by Wendelken and Ulehla (1979). It is more likely that this shift with increase in coverage is due to two different linear sites such as the C_6 and C_{10} sites. These workers also find a loss peak at 686 cm^{-1} at low coverages, the origin of which is not clear to us.

Thomas and Weinberg (1979a) find only one C–O stretching frequency due to linear CO on Ru(001) in agreement with infrared results. The position of this band, however, seems to vary with coverage. There appears to be some LEED evidence for the presence of sites of lower symmetry on the Ru(001) surface, but it is not clear how the observed CO frequencies can be rationalized with the LEED data. Thomas and Weinberg (1979a) have considered a model which is insensitive to the registry of CO. On Rh(111) surface, both linear and bridged CO species have been identified based on high resolution EELS and other data (Dubois and Somorjai, 1980). The linear CO stretching band at 1990 cm^{-1} at low coverage is shifted to 2070 cm^{-1} with increasing coverage. The C–O stretching force constants are 16.5×10^2 N/M and 13.3×10^2 N/M for the linear and bridge sites respectively, the corresponding M–C stretching force constants being 2.40×10^2 and 2.38×10^2 N/M.

Adsorption of CO becomes dissociative on W surfaces at low coverages; at high coverages, however, molecular adsorption occurs. On W(100), a linear CO frequency of 2080 cm^{-1} has been reported, while on W(111) and (110) surfaces, a band at 1993 cm^{-1}

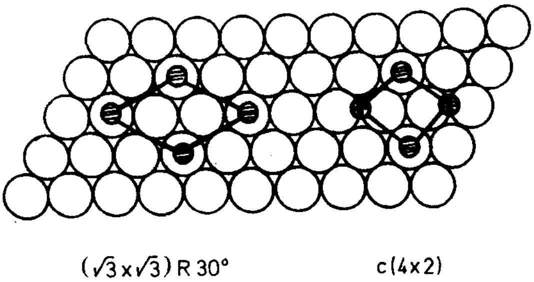

$(\sqrt{3} \times \sqrt{3})$ R30°　　c(4x2)

FIG. 3. Geometrical structure model for the $(\sqrt{3} \times \sqrt{3})$ R30° and c(4 × 2) structure of CO on Pt(111) (after Hopster and Ibach, 1978).

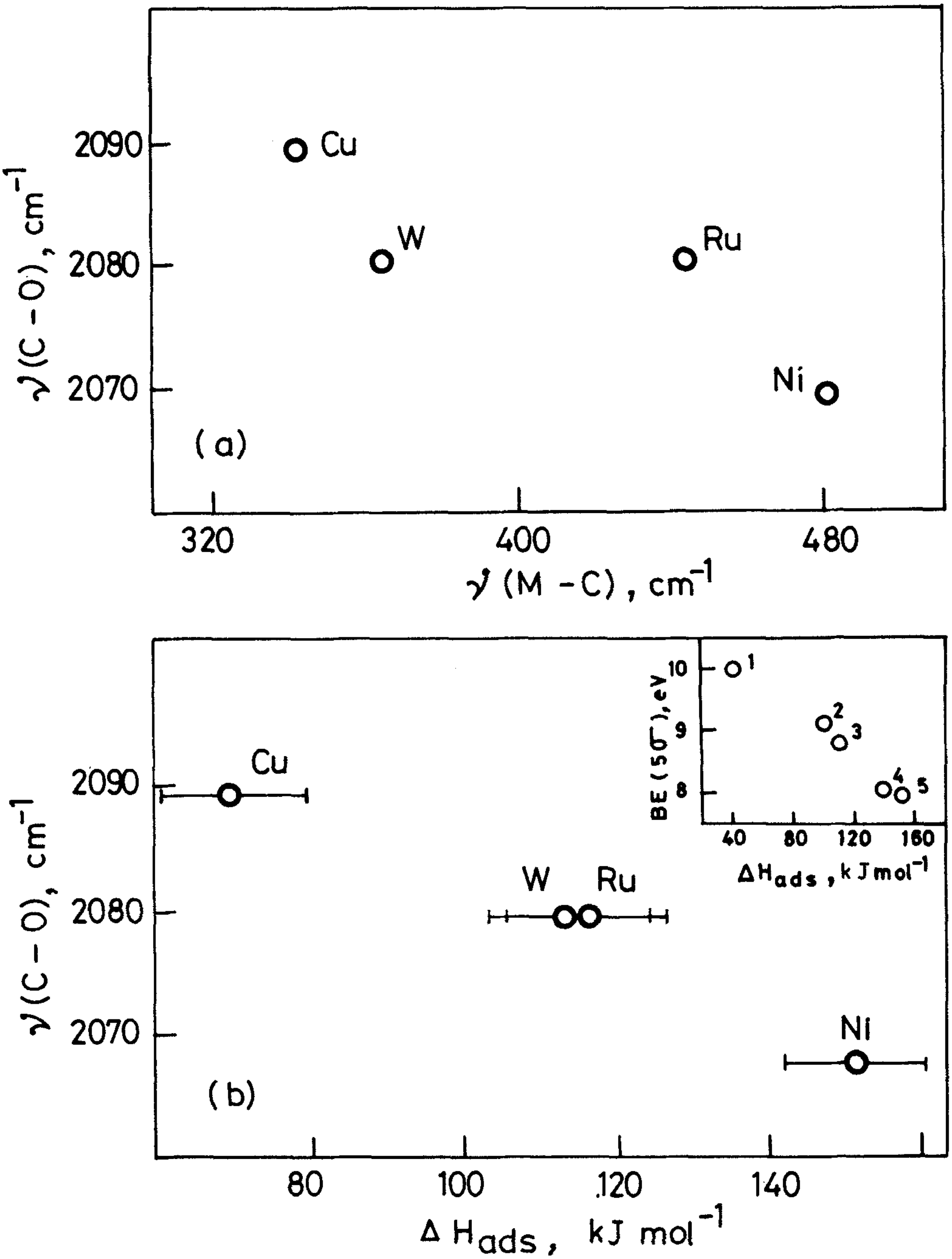

FIG. 4. (a) Plot of the C–O stretching frequency of carbon monoxide adsorbed on metal (100) surfaces against the metal-carbon (M–C) stretching frequency. (b) Plot of the C–O stretching frequency of carbon monoxide adsorbed on metal (100) surfaces against the heat of adsorption (after Rao, Srinivasan and Jagannathan, 1981). The values of heats of adsorption are taken from Somorjai (1979). Inset shows the variation of 5σ(CO) binding energy with the heat of adsorption; 1, Cu(311); 2, Pt(100); 3, W(100) and Ni(111); 4, Ni(110); 5, Pd(100) and Ni(100) (after Rao, Srinivasan and Jagannathan, 1981).

characteristic of a B_2 site has been reported (Froitzheim, Ibach and Lehwald, 1977; Backx *et al.*, 1977b). The results are essentially in good agreement with those from infrared spectroscopy. The W–C stretching frequency is lower for the (100) surface than for (110) or (111) surfaces. When CO is dissociatively adsorbed, characteristic frequencies due to W–C and W–O stretching modes are observed at 548 and 629 cm^{-1} respectively (Froitzheim, Ibach and Lehwald, 1977).

The observed C–O stretching and M–C stretching frequencies of the linear species on metal (100) surfaces are found to be inversely related to each other (*Fig. 4a*). That is, for a given metal, the higher the C–O stretching frequency, the lower is the M–C stretching frequency implying that as the M–C bond becomes stronger, the C–O bond becomes weaker. This trend is not observed in the case of Ni(111) and Pt(111) surfaces where the C–O stretching frequencies are 2047 and 2088 cm^{-1} respectively with the corresponding M–C frequencies at 403 and 475 cm^{-1}. We find no simple relationship between C–O and M–C stretching frequencies of bridged B_2 species. Also, no separate asymmetric and symmetric metal–carbon stretching frequencies (due to B_2 species) have been reported in most of the systems. The C–O stretching frequency of the linear site on metal (100) surfaces decreases with the increase in the heat of adsorption as one would expect (*Fig. 4b*); the C–O stretching and the M–C stretching frequencies also vary systematically with the surface potential. It is interesting that the binding energy of the 5σ level of CO obtained from UV photoelectron spectroscopy also decreases with increase in the heat of adsorption (*Fig. 4b*).

Dissociative chemisorption of CO_2 on Rh(111) surface has been studied by Dubois and Somorjai (1979 and 1980) who report two C–O stretching frequencies around 1870 and 2070 cm^{-1} due to bridge and linear CO species respectively (*Table 3*). The C–O and the M–C stretching frequencies due to the linear CO species on Rh(111) fit well with those of Ni(111) and Pt(111) surfaces discussed earlier. On these three surfaces, the C–O and M–C stretching frequencies increase in the same direction unlike the (100) surfaces (*Fig. 4a*).

MSX_α calculations of oriented molecules on metals have been carried out by Davenport, Ho and Schrieffer (1978). The differential cross section for the excitation of single adsorbate interaction (in the case of CO) has been calculated for electrons specularly reflected (Newns, 1977). A comparison of the absolute intensities both from high resolution EELS and infrared adsorption has been made by Ibach (1977) for CO on Pt(111) and good agreement has been found. The frequencies and amplitudes of CO vibrations on metal surfaces have been estimated from model cluster calculations by Richardson and Bradshaw (1979). The 'best fit' stretching force constants F_{Ni-C} and F_{C-O} are 2.6×10^2 and 16.8×10^2 N/M for linear CO and 1.1×10^2 and 14.9×10^2 N/M for bridged CO. These values are in good agreement with those of Andersson (1977a). The amplitudes of bending modes have also been calculated (Richardson and Bradshaw, 1979); these amplitudes are strongly temperature-dependent. The dependence of the CO stretching frequency adsorbed on metals on surface coverage has been interpreted in terms of dipole interactions (Mahan and Lucas, 1978); dipole interactions provide a shift of about 10 cm^{-1} which is about one third of the value found experimentally.

Nitric Oxide

On Pt(111) surface (at 160 K), nitric oxide is adsorbed linearly giving rise to losses at 306 and 1515 cm^{-1} due to Pt–N and N–O stretching vibrations (Ibach and Lehwald, 1978b). At higher coverages, peaks are seen at 306, 451 and 1717 cm^{-1} due to Pt–N stretching, Pt–NO bending and N–O stretching due to a state corresponding to the dimer.

This dimer model has been preferred to a simple C_{2v} state by Ibach and Lehwald (1978b).

On Ru(001) surface, Thomas and Weinberg (1978) find evidence for linear and bridged NO species at 130 K. These workers find a peak between 1411 and 1508 cm^{-1}, the frequency of which increases with coverage. At higher coverages, they see a band around 1830 cm^{-1} which is attributed to linear NO. The 1411–1508 cm^{-1} band is attributed to a 3-fold bridged site. Ru–N stretching frequencies are found in the range 512–560 cm^{-1}. Bridged NO appears to dissociate completely at 316 K. Thiel, Weinberg and Yates (1979a) have also investigated the adsorption of NO on Ru(001) and attribute a peak at 1379–1525 cm^{-1} to a 2- or 3-fold bridge site and a peak at 1783–1823 cm^{-1} to linear NO at high coverages. A transient species with a loss peak at 1160 cm^{-1} has also been observed by these workers. Linear NO shows a metal–nitrogen frequency around 540 cm^{-1}.

Acetylene

Adsorption of C_2H_2 on metal surfaces has been investigated by several workers. One of the most important conclusions from these studies is that there is rehybridization of the adsorbed molecule resulting in the lowering of the C–C bond order. The important information obtained from high resolution EELS studies are presented in *Table 4*. We see that on all the metal surfaces studied, there is considerable lowering of the C–C stretching frequency of acetylene, the maximum lowering being in the case of Ni(111) (Lehwald and Ibach, 1979).

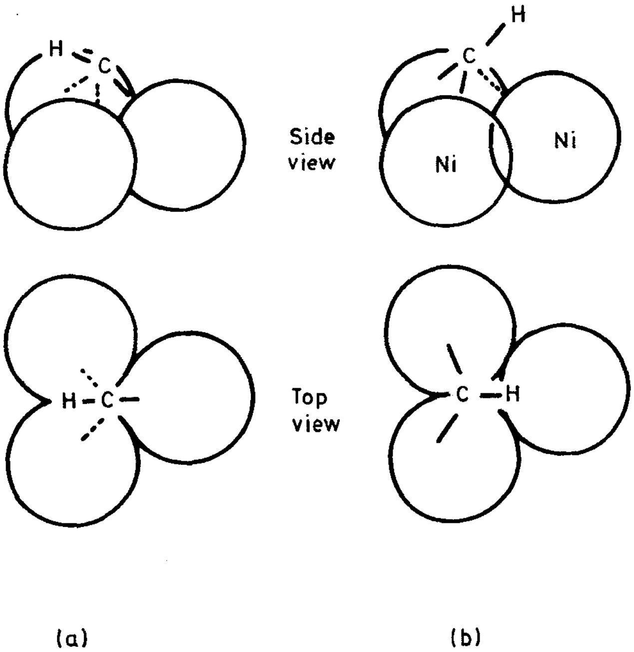

FIG. 5. Schematic diagram of two possible bonding geometries for CH species on Ni(111) as deduced from the vibrational loss spectra. Model (a) and (b) correspond to *sp* and sp^2 hybridized species respectively. A weak interaction between the hydrogen in CH and surface Ni atoms may also occur (after Demuth and Ibach, 1978).

TABLE 4. Vibrational spectra of acetylene adsorbed on metals

Surface	Ep (eV)	Temperature (K)	Coverage	Energy loss peaks (cm^{-1})	Remarks	Reference
Ni(111)	4.2	300	3 L C_2H_2	2910, ν(C–H); 1200; ν(C–C); 870, δ(C–H); 500, ν(Ni–C)		Lehwald and Ibach, 1979
			C_2D_2	2190, ν(C–D); 1195, ν(C–C); 650, δ(C–D); 470, ν(Ni–C)		
Ni(111)	2	300	<1.5 L C_2H_2	2942, ν(C–H); 1217, ν(C–C); 854, δ(C–H); 484, ν(Ni–C)		Bertolini, Massardier and Dalmai-Imelik, 1978
			10 L	2942, 1217, 854, 685, 314, 1088, 999, 774		
Ni(111)	4.2	>400 500	18 L CH	2980, ν(C–H); 790, δ(C–H); 540, ν(Ni–C)	Also at 1300 due to another CH_2 species	Lehwald and Ibach, 1979
Ni[5(111) × ($\bar{1}$10)]	4.2	150	0.6 L C_2H_2	2920, ν(C–H); 1200, ν(C–C); 870, δ(C–H)	Also at 690 due to adsorbed hydrogen	
			C_2	2220, ν(C–C); 550, ν(C); 350, ν(Ni–C)		
Pt(111)	4–5	300	2 L C_2H_2	3010, ν(C–H); 1310, ν(C–C); 985, δ(C–H); 770, γ(C–H); 570, ν(Pt–C)$_\pi$; 340, ν(Pt–C)$_\sigma$		Ibach, Hopster and Sexton, 1977; Ibach and Lehwald, 1978a
Rh(111)	4	<270	2 L	3085, ν_a(C–H); 2985, ν_s(C–H); 1300–1400, ν(C–C); 887, δ(C–H); 706, δ(C–H); 323, ν(Rh–C)		Dubois, Castner and Somorjai, 1980
W(110)	4	300	0.5 L C_2H_2	2926, ν(C–H); 1265, ν(W–H); 564, ν(W–C) of (CH) species	Dissociated C_2H_2	Backx and Willis, 1978
			1 L 2 L	Additional losses 1435, $\delta(CH_2)$; 927, δ(C–H); 2926, ν(C–H); 1128, ν(C–C); 927, δ(C–H); 580, ν(W–C)	CH_2–W_2 complex, $CHW_3 + HW_2CCW_2H$	

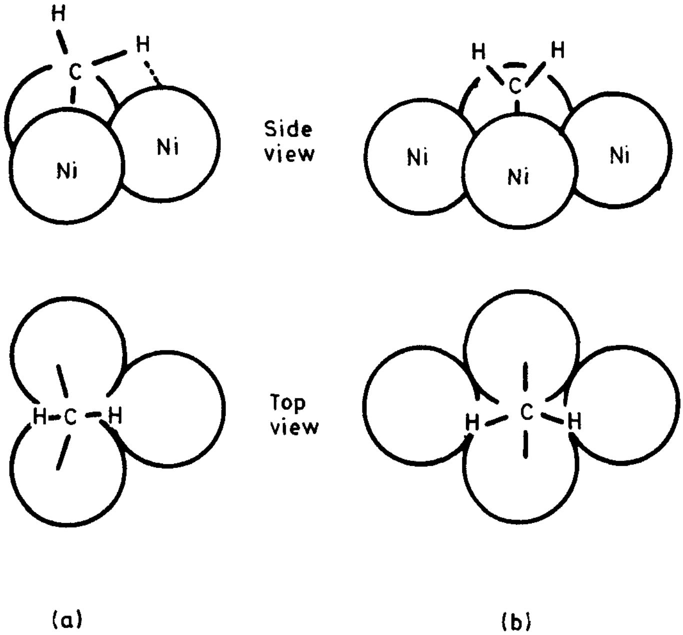

FIG. 6. Schematic diagram of two possible geometries for the CH_2 species as inferred from the vibrational loss spectra. The dashed bond represents a possible interaction between the hydrogen atom and the substrate (after Demuth and Ibach, 1978). (a) Plane of molecule perpendicular to surface, (b) plane of molecule skewed with respect to surface.

Lehwald and Ibach (1979) report energy loss peaks at 2910 (C–H str), 1200 (C–C str), 870 (C–H bend) and 500 cm^{-1} (Ni–C str) when C_2H_2 is adsorbed on Ni(111) surface at 300 K. Above 400 K, a C–H stretching frequency of 2980 cm^{-1} and a bending frequency at 790 cm^{-1} are found. This feature is identified with a surface stabilized CH radical (*Fig. 5*). Upon warming this to 450 K, another loss peak near 1300 cm^{-1} is observed which intensifies on further heating. This has been attributed to CH_2 formed by the self hydrogenation of the CH species (*Fig. 6*). Heating to 500 K only results in surface carbon atoms with a Ni–C frequency at 540 cm^{-1}. It appears that in the case of the Ni(111) surface, the two carbon atoms lie above two adjacent three-fold sites with the C–C bond axis slightly skewed relative to the surface, the plane of the molecule itself being normal to the surface (Demuth and Ibach, 1979b; Lehwald and Ibach, 1979). Hybridization of carbon in acetylene adsorbed on Ni(111) is estimated to be somewhere between $sp^{2.5}$ and sp^3.

On a stepped Ni[5(111) × ($\bar{1}$10)] surface, two new bands at 2220 cm^{-1} and 350 cm^{-1} are found and these are ascribed by Lehwald and Ibach (1979) to C_2 which essentially retains the triple bond. These workers suggest that the stepped Ni surface is considerably more reactive for the decomposition than the flat surface.

On W(110) surface, Backx and Willis (1978) find that C_2H_2 decomposes giving rise to a new C–H species at low coverages; adsorption is however associative at high coverages. The C–C stretching frequency on this surface is only 1120 cm^{-1} which is considerably lower than that found on other surfaces. It is rather surprising that the C–H stretching frequency of adsorbed C_2H_2 on W(110) is only 2926 cm^{-1}. The degree of back bonding from the metal *d*-state determines, generally, the amount of C–C stretch and C–H bond bending as illustrated in *Fig. 7a*. On the other hand the 2926 cm^{-1} loss peak

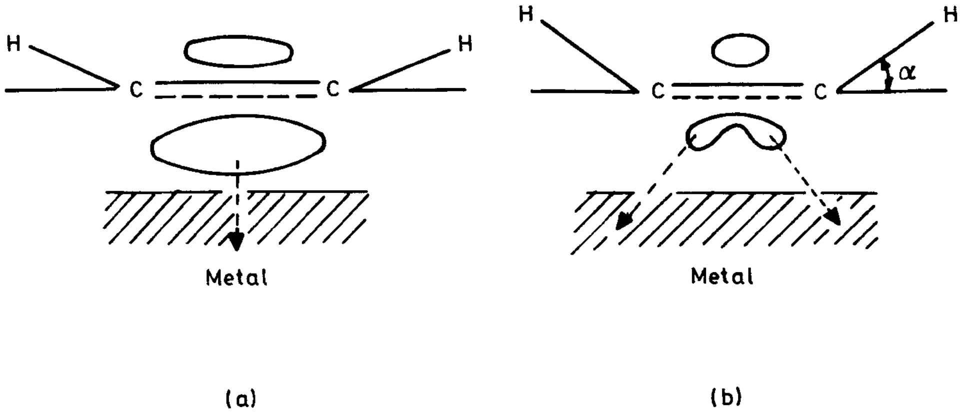

FIG. 7. Molecular orbital geometrics and charge densities for (a) π–d bonded C_2H_2 and (b) an 'olefinic' chemisorbed di σ-like complex produced by rehybridization of the molecular orbitals with d-states; charge donation occurs to the metal via the molecular π-orbitals with back-donation into the antibonding orbitals from the metal (after Backx *et al.*, 1977b).

is typical of a sp^3 C–H stretching vibration, indicating that a di–σ bonding mechanism might be more applicable in the case of W(110) (*Fig. 7b*).

The C–H stretching as well as C–C stretching frequencies (3010 and 1310 cm^{-1} respectively) are highest in the case of Pt(111) surfaces (Ibach, Hopster and Sexton, 1977; Ibach, Lehwald and Sexton, 1977; Ibach and Lehwald, 1978a). The bonding geometry of C_2H_2 on Pt(111) appears to differ significantly from that on Ni(111) (Demuth and Ibach, 1979b). In the case of Pt(111), the carbon atoms lie along a line parallel to the surface and the molecular plane of C_2H_2 is inclined at an angle to the surface. Thus, there is less rehybridization on Pt(111) than on Ni(111) (*see Fig. 8*). While a vinyl-like species seems to be present on Pt(111) above 300 K, on Ni(111) surface C_2H_2 dissociates above 400 K.

Dubois, Castner and Somorjai (1980) find that C_2H_2 chemisorbs on Rh(111) surface with the C–C bond parallel to the surface forming sp^2 hybridized species; LEED studies show this to have a (2 × 2) structure just as with C_2H_4. In the range 270–300 K range, a c(4 × 2) hydrocarbon overlayer is formed both by C_2H_2 and C_2H_4, addition of hydrogen to C_2H_2 being necessary to complete such a transformation. The stable hydrocarbon species formed by $C_2H_2 + H_2$ and C_2H_4 on Rh(111) is similar to that formed on a Pt(111) surface.

The C–C π-bond orders of adsorbed C_2H_2 molecules can be estimated using the stretching frequencies of the C–H and C–C bonds as shown in *Fig. 9*. It can be seen that the π-bond orders of adsorbed C_2H_2 are less than 0.5. The estimated π-bond orders on different surfaces vary in the order W(110) < Ni(111) < Pt(111). These results clearly establish that rehybridization of C_2H_2 occurs on adsorption.

Earlier infrared studies on the adsorption of acetylene on metal surfaces have been reviewed by Little (1966). Adsorption of C_2H_2 on supported metals was studied by Little, Sheppard and Yates (1960) who found evidence for $=CH_2$ groups on the surface because of the bands at 3090 cm^{-1} (asymmetric stretching of CH_2 groups). A band at 3030 cm^{-1} was assigned to the $>CH$ group. Infrared studies of C_2H_2 adsorbed on Ni and Pt surfaces show that the C–H stretching frequencies are in the range of 3150–3225 cm^{-1}, while the C–C stretching frequencies are in the range of 1800–1900 cm^{-1}. Using infrared reflection

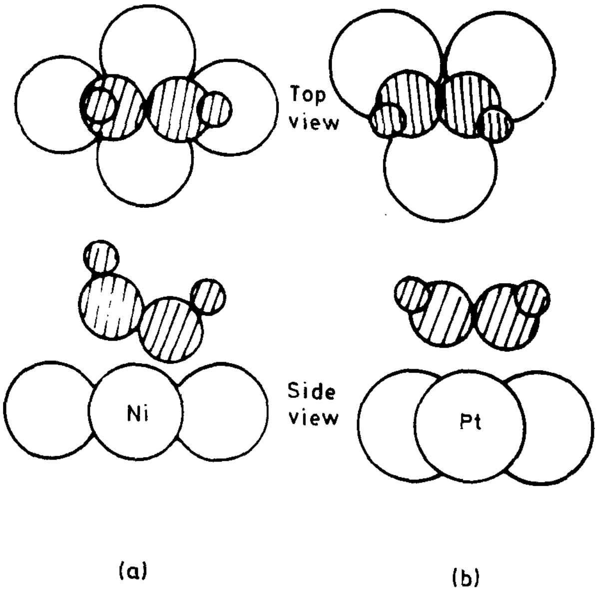

FIG. 8. Bonding geometry and molecular orbital orientation for (a) C_2H_2 on Ni(111) and (b) C_2H_2 on Pt(111). For geometry (a) the hydrogen atoms are bent strongly away from the C–C axis and the two carbon atoms lie at slightly different heights above the surface. (The molecular plane of acetylene is normal to the surface.) For geometry (b) the carbon atoms lie along a line parallel to the surface while the molecular plane of acetylene is inclined at some angle to the surface (after Demuth and Ibach, 1979b).

technique, Ito and Süetaka (1977a and b) find vibrational bands at 3300 and 3225 cm^{-1} (νCH), 1900 cm^{-1} (νCC), 760 cm^{-1} (γCH) and 510 cm^{-1} (νPt–C), the last three being doublets when C_2H_2 is adsorbed on Pt suggesting two acetylenic species on the surface. On Ni surface, these workers find bands at 3150 (C–H symmetric stretching), 1800 (C–C stretching), 850 (HCC deformation) and 495 cm^{-1} (M–C symmetric stretching) for strongly chemisorbed C_2H_2. The C–H stretching frequencies due to adsorbed C_2H_2 found by high resolution EELS are generally much lower than those found from infrared studies. Recently, Krasser, Fadini and Renouprez (1980) have reported Raman spectra of C_2H_2 adsorbed on Ni/SiO_2 and find a band around 2980 cm^{-1} due to C–H stretching at high coverages; the position of this as well as the other bands agree well with the high resolution EELS data of Demuth and Ibach (1979b).

Ethylene

High resolution EELS studies on ethylene adsorbed on the Ni(111) and Pt(111) surfaces are summarized in *Table 5*. The data on Ni(111) clearly show evidence for saturated species involving rehybridization of the molecule. Thus, the C–H stretching frequency of adsorbed C_2H_4 is found around 2945 cm^{-1}; unlike the case of C_2H_4, both the symmetric and asymmetric stretching frequencies are resolved in the case of C_2D_4 and these are found at 2170 and 2270 cm^{-1} respectively (Lehwald and Ibach, 1979). An interesting feature noted by Lehwald and Ibach (1979) is the peak around 2740 cm^{-1} at high coverages due to 'hydrogen bonding' of the molecule to the Ni(111) surface. All the energy loss data on

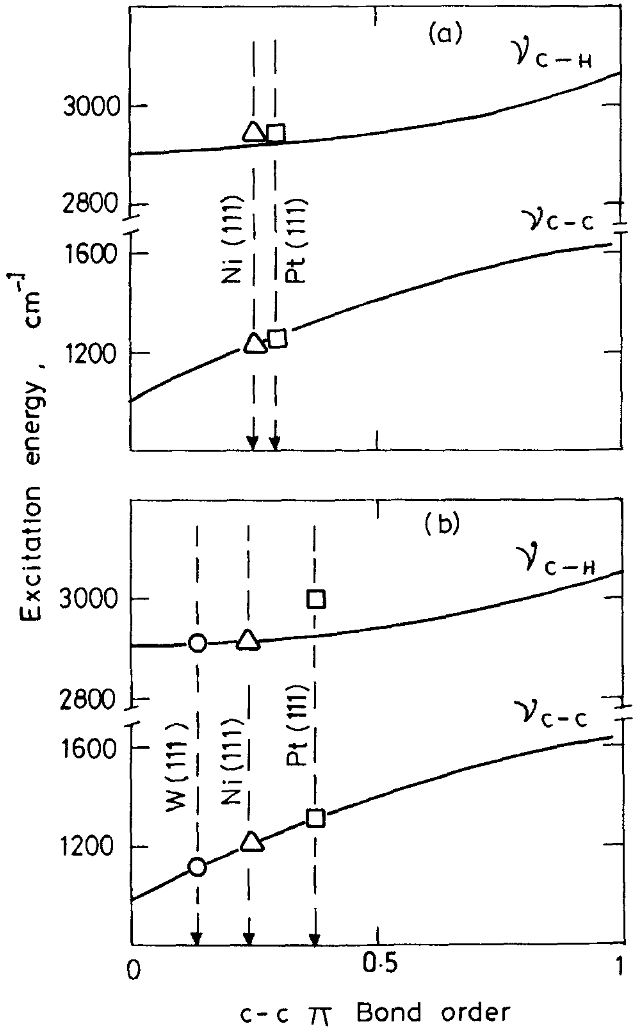

FIG. 9. Plots of C–H and C–C stretching frequencies of (a) ethylene and (b) acetylene adsorbed on metal surfaces against the C–C π-bond order.

the adsorption of C_2H_4 seem to be consistent with a di–σ bonded molecule, with a C_s or C_1 symmetry at high coverages. A good comparison of the energy loss-spectra of C_2H_4 on Ni(111) surfaces can be made with the infrared data on $C_2H_4Br_2$ in the gauche form. The spectrum of C_2H_4 on Ni(111) at 230 K is similar to that of C_2H_2 in the presence of coadsorbed hydrogen, the latter giving rise to a 500 cm^{-1} band. The estimated π-bond orders of adsorbed C_2H_4 molecules (as seen from *Fig. 9*) are less than 0.5.

On a stepped $Ni[5(111) \times (\bar{1}10)]$ surface, adsorption of C_2H_4 is rather more complicated. The asymmetric and symmetric C–H stretching frequencies are found around 3000 and 3100 cm^{-1} suggesting that there is no rehybridization on the stepped surface. Accordingly, the C–C stretching frequency is found around 1500 cm^{-1}. There is also some evidence for the presence of more than one adsorbed phase on a stepped surface. With increase in temperature, decomposition occurs via a sp^3 type hybridized species as evidenced by C–H stretching bands around 2950 cm^{-1}.

On a Pt(111) surface, Ibach and Lehwald (1978a) have proposed the formation of an ethylidene, $>CH-CH_3$, species at room temperature (300 K) on the basis of the high resolution EELS data. Kesmodel, Dubois and Somorjai (1978) have given reasons for believing that the stable species formed from the chemisorption of C_2H_4 as well as C_2H_2 on Pt(111) above 300 K is ethylidyne, $\gg C-CH_3$, rather than ethylidene, $>CH-CH_3$, species. These workers have analysed both LEED and energy loss data based on this species. The overall reaction can be written as follows:

$$C_2H_2(g) + H^* \longrightarrow \ \gg C-CH_3$$

$$C_2H_4(g) \longrightarrow \ \gg C-CH_3 + H^*$$

Demuth (1979) has, however, shown that a partially dehydrogenated species of the composition C_2H_3 (vinyl species, $-CH=CH_2$) is formed on Pt(111) around 300 K on the basis of UVPS and thermal desorption studies. Demuth (1980) later points out that the high resolution EELS data of Ibach, Lehwald and Sexton (1977) and Ibach and Lehwald (1978) can be reinterpreted in terms of multiply bonded $CH-CH_2$ species which would also be fairly consistent with the LEED data (a simple vinyl species not being satisfactory in this regard (*Fig. 10*). He suggests that σ bonds form to both the carbon atoms and that one of the C-atoms is multiply coordinated in a high coordination site and lies closer to the surface. This model also explains the separation of symmetric and asymmetric CH_2 stretching modes on deuteration. However, we feel that there is sufficiently strong evidence for a surface species containing $C-CH_3$ group (either ethylidene or ethylidyne type) and the actual nature of this species is not altogether firmly established. The C–C π-bond orders of ethylene adsorbed on different surfaces can be estimated from the C–H and C–C stretching frequencies as in *Fig. 8*. The π-bond order on Pt(111) is greater than on Ni(111) just as in the case of acetylene.

Adsorption of C_2H_4 on metals has been studied by infrared spectroscopy and in the case of Ni on silica two C–H stretching bands at 2960 and 2870 cm^{-1} have been observed on a hydrogen-covered surface by Little, Sheppard and Yates (1960). Based on this observation they propose saturation of the species on the surface. Morrow and Sheppard (1969) find three dominant peaks at 2920, 2880 and 2795 cm^{-1} in the infrared spectra of chemisorbed ethylene on silica supported Pt, the corresponding bands on Ni being at 2920, 2870 and 2790 cm^{-1}. They ascribe these to the species MCH_2-CH_2M

TABLE 5. Vibrational spectra of ethylene adsorbed on metals

Surface	Ep (eV)	Temperature (K)	Coverage	Energy loss peaks (cm^{-1})	Remarks	Reference
Ni(111)	4.2	150	0.5–3 L C_2H_4	2950, ν_s(C–H); 1440, CH_2 sciss; 1200, ν(C–C); 1100, CH_2 wag; 880, CH_2 twist; 720, CH_2 rock; 610, ν(Ni–C); 450, ν(Ni–C)	2740 band only at 3 L rehybridization to a saturated species indicated	Lehwald and Ibach, 1979 Demuth, Ibach and Lehwald, 1978
			C_2D_4	2270, ν_a(C–D); 2170, ν_s(C–D); 1200, CD_2 sciss; 870, CD_2 wag; 740, CD_2 twist; 650, CD_2 rock; 590, (Ni–C); 420, (Ni–C)	2020 band only at 3 L	
	4.2	230	3 L C_2H_4	Spectrum similar to coadsorbed (H_2 + C_2H_2)		
	2	300	6 L C_2H_4	2942, ν(C–H); 1217, ν(C–C); 854, CH_2 twist; 685, CH_2 rock; 484, ν(Ni–C) and 315, ν(Ni–C)		Bertolini and Rousseau, 1979a
Ni[5(111) × ($\bar{1}$10)]	4.2	150	3 L C_2H_4	3000, ν_s(C–H); 3100, ν_a(C–H); 1510, ν(C–C); 1420, 1200, 900, 610 and 350 only partial assignments possible. Decomposition at higher temps. to C_2H_2 via a *sp*^{3}-type species (with ν(C–H) ~ 2950)		Lehwald and Ibach, 1979
Pt(111)	5	140	3 L C_2H_4	2940, ν_s(C–H); 1420, CH_2 sciss; 1230, ν(C–C); 990, CH_2 wag; 790, CH_2 twist; 470, ν(Pt–C)	Rehybridization to a saturated species indicated	Ibach, Hopster and Sexton, 1977; Ibach and Lehwald, 1978a; Lehwald and Ibach, 1979
			C_2D_4	2275, ν_a(C–D); 2160, ν_s(C–D); 1150, CD_2 sciss; 890, CD_2 wag; 740, CD_2 twist; 440, ν(Pt–C)		
	5	300	3 L C_2H_4	3045, 2920, 1420, 1355, 1130, 900	CH CH_2, C CH_3 or $CHCH_3$ species	Demuth, 1980

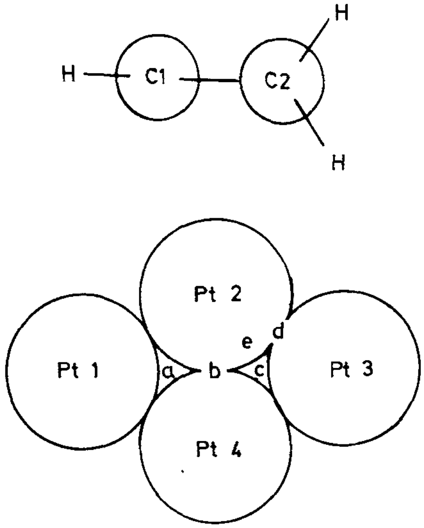

	Model			
	1	2	3	4
Atom C_1	a	b	a → b	a/b
Atom C_2	e	d	e → d	d/f

Fig. 10. Schematic diagram and labelling convention for the CH–CH_2 species and possible bonding sites on a Pt(111) surface. Model configurations for CH–CH_2 on a Pt(111) surface as per locations and atom designations given in the schematic diagram are shown in the table. Here → indicates any location intermediate between two end points, a/b indicates between a and b (after Demuth, 1980).

and attribute a weaker band at 3010 cm^{-1} to a surface MCH = CHM complex. These authors also suggest that there is considerable initial dissociative chemisorption at higher temperatures (270–320 K). A band at 2907 cm^{-1} due to $M_2CH–CHM_2$ is found at 130 K. All the spectroscopically observable species have been attributed to σ bonding to metal surfaces rather than π bonding. Prentice, Lesiunas and Sheppard (1976) have reported evidence for π-bonded species from ethylene chemisorbed on silica supported Pt and Pd catalysts with characteristic infrared bands at 1500 cm^{-1} and 3000 cm^{-1}. These species co-exist with σ bonded $CH_2M–MCH_2$ species but are more readily removed on interaction with hydrogen.

Ito and Süetaka (1977a) find a broad band around 1000 cm^{-1} due to C–H bending on Pt(111). They also find bands around 3300, 3200, 2950 and 2750 cm^{-1}. Of these, the first two are ascribed to acetylene, the 2950 cm^{-1} band to adsorbed C_2H_4 and the 2750 cm^{-1} band to a saturated species. They suggest that C_2H_4 is deformed (C_{2v} symmetry) on the Pt surface. On Ag surface these workers find bands at 3300, 2900 and 2600 cm^{-1} due to C–H stretching and a band at 960 cm^{-1} to a C–H bending mode. The infrared frequencies observed by these workers do not agree with the data on dispersed

TABLE 6. Vibrational spectra of cyclohexane adsorbed on metals

Surface	Ep (eV)	Temperature (K)	Coverage	Energy loss peaks (cm^{-1})	Remarks	Reference
Ni(111)	4.5	150	5 L	2900 (2930, 2852), ν(C–H); 2720 (broad), hydrogen bonded species; 1460 (1465, 1437, 1457); 1260 (1261); 1020 (1030); 900 (907, 863); 520 (523); 390 (383)	Band positions in parenthesis are from infrared spectroscopy	Demuth, Ibach and Lehwald, 1978; Lehwald and Ibach, 1979
Ni[5(111) × ($\bar{1}$10)]	4.5	150	3 L	2910 (all bands as above); 1450 1330 (addnl. band); 1260, 1040, 850, 540, 400; no band at 2720	Partial dehydrogenation	Lehwald and Ibach, 1979
Pt(111)	5	140	3 L	2900, ν(C–H); 2590, hydrogen bonded species; 1440, 1260, 1160, 1030, 870, 520 and 370		Demuth, Ibach and Lehwald, 1978

metal surfaces. It is possible that surface sites are different in the two situations. It is still somewhat surprising that the energy loss peaks due to ethylene adsorbed on metals do not exactly agree with those found from infrared spectroscopy. There are fewer peaks in the C–H region in the energy loss spectrum. It is certainly worthwhile to carry out a comparative study of the energy loss and infrared spectra of adsorbed ethylene as well as of acetylene.

Cyclohexane

Cyclohexane adsorbed on a smooth Ni(111) surface gives energy loss peaks which can be readily interpreted by comparison with infrared data of the free molecule (Lehwald and Ibach, 1979). However, an additional loss peak is found around 2720 cm^{-1} due to 'hydrogen bonding' (*Table 6*). All the observed bands of C_6H_{12} on Ni(111) surface have been interpreted by Lehwald and Ibach (1979) in terms of the molecule with its ring not parallel to the surface (C_s symmetry). On a stepped Ni $[5(111) \times (\bar{1}10)]$ surface, all the peaks of cyclohexane with the exception of the 2720 cm^{-1} peak are observed. Low intensity losses found around 2620 cm^{-1} suggest additional H atom surface interaction (hydrogen bonding) as in the case of C_2H_4. Some bands are found on the stepped surface due to dehydrogenation even at 150 K. Between 200 and 250 K bands due to benzene are observed on the stepped surface.

Benzene

Results from high resolution EELS studies of benzene adsorbed on Ni(100), (111) and Pt(111) surfaces are shown in *Table 7*. Bertolini, Dalmai-Imelik and Rousseau (1977a) and Bertolini and Rousseau (1979b) report that the aromatic character of benzene is retained on the surface with the molecule π-bonded to the surface with the ring parallel to it; there appears to be no evidence for any difference in the configuration of the adsorbed species on Ni(100) and Ni(111) surfaces. Chemisorption induces the ordered structures c(4 × 4) on Ni(100) and $(2\sqrt{3} \times 2\sqrt{3})$ R 30° on Ni(111). In preserving its aromatic character, benzene involves eight Ni surface atoms on the (100) surface and twelve on the (111) surface (Bertolini, Dalmai-Imelik and Rousseau, 1977a). Bertolini and Rousseau (1979b) assign the 1425 and 1325 cm^{-1} losses to C–C bending vibrations; we feel that they are likely to be due to C–C skeletal stretching vibrations which characteristically appear in the 1400–1600 cm^{-1} region in free benzene derivatives.

In the case of Pt(111), there is a significant increase in the C–H out of plane bending mode as compared to the free molecule (Lehwald, Ibach and Demuth, 1978). On both Pt(111) and Ni(111) surfaces, two phases of benzene have been found by Lehwald, Ibach and Demuth (1978) with characteristic frequency shifts; these shifts have been explained on the basis of electronic interaction between the metal *d* orbitals and the molecules adsorbed in two different (on-top and three-fold hollow) sites. A multilayer condensed phase of benzene shows infrared active modes of the gas phase molecule.

In *Fig. 11* we have plotted the ν(M–C) against ν(C–H) as well as ν(C–C) stretching frequencies of acetylene, ethylene and benzene adsorbed on Ni(111) and Pt(111) surfaces; the plots are quite linear as one would expect.

Water

Vibrational spectra of water adsorbed in submonolayer and multilayer quantities on Pt(100) have been investigated by Ibach and Lehwald (1980) who find the spectrum of adsorbed multilayers to be similar to that of ice I. Submonolayers show OH stretching

TABLE 7. Vibrational spectra of benzene adsorbed on metals

Surface	Ep (eV)	Temperature (K)	Coverage	Energy loss peaks (cm^{-1})	Remarks	Reference
Ni(100)	2	300	3 L	3047, ν(C–H); 1439, δ(C–C); 1340, δ(C–C); 1128, δ(C–H); 850, ν(C–C); 754, γ(C–H); 363, ν(M–C)		Bertolini and Rousseau, 1979b
Ni(111)[a]	2	300	3 L	3047, ν(C–H); 1439, δ(C–C); 1340, δ(C–C); 1128, δ(C–H); 850, ν(C–C); 754, γ(C–H); 292, ν(M–C)		
Ni(111)[a]	4.2	280	2 L	3022, 1445, 1144, 825, 734 and 323	Bands assigned as above	Lehwald, Ibach and Demuth, 1978
Pt(111)[a]	5	300	0.4 L	3022, ν(C–H); 1434, δ(C–C); 1143, δ(C–H); 926, γ(C–H); 835, γ(C–H); 574, $\nu(Pt–C)_\pi$; and 363, $\nu(Pt–C)_\sigma$		Lehwald, Ibach and Demuth, 1978
			0.9 L	2257, ν(C–D); 1358, δ(C–D); 805, δ(C–D); 705, γ(C–D); 614, γ(C–D) and 353, ν(C–Pt)		

[a] The bands in the region 1340–1440 cm^{-1} are probably due to skeletal stretching modes. We have used these frequencies in the correlation shown in *Fig. 11*.

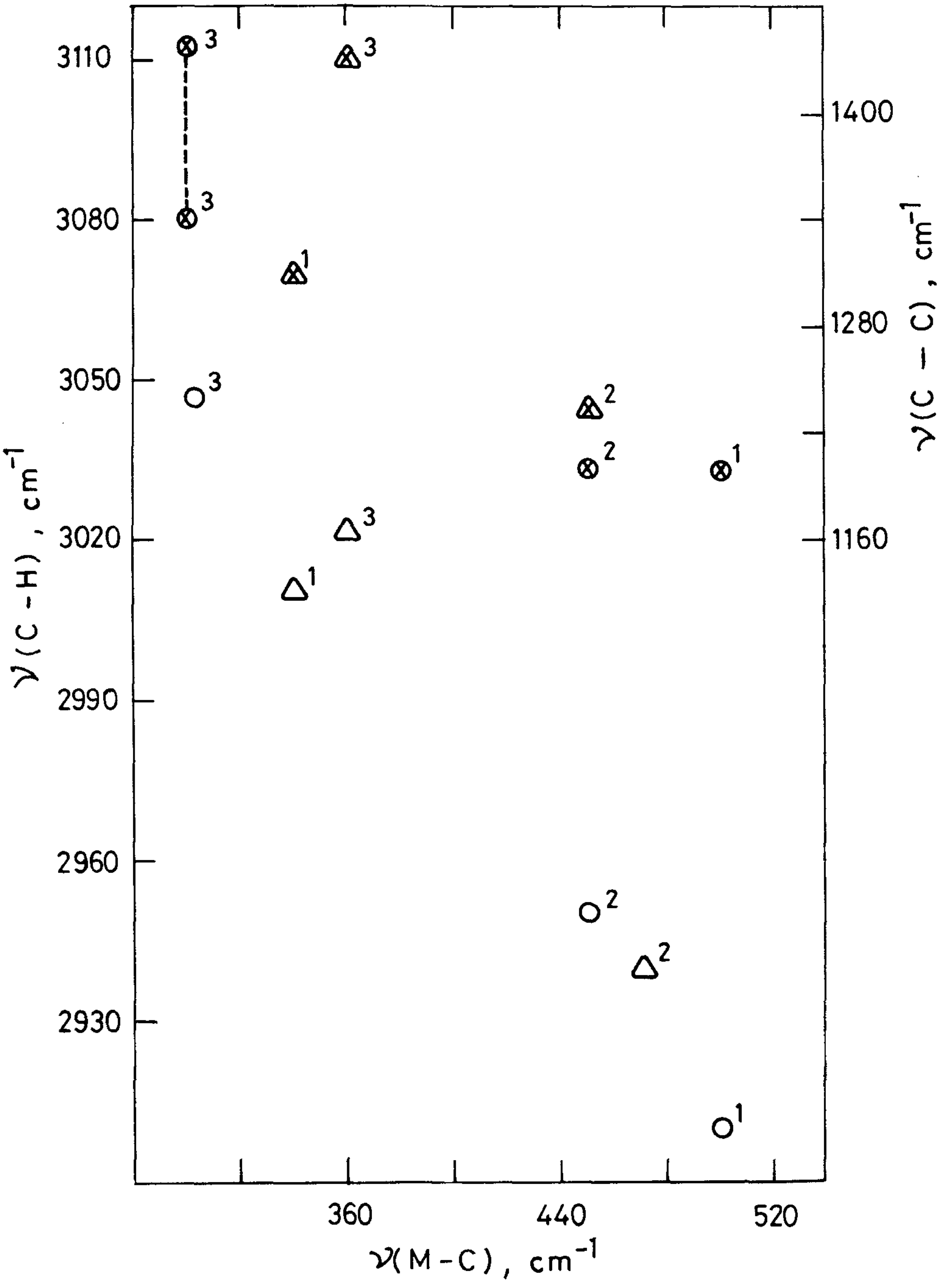

Fig. 11. Correlation of metal–carbon (M–C) stretching frequencies with C–H and C–C stretching frequencies of acetylene (1), ethylene (2) and benzene (3) adsorbed on Ni(111) and Pt(111) surfaces. The C–H stretching frequencies are denoted by O(Ni) and △ (Pt) while the C–C stretching frequencies are denoted by ⊗ (Ni) and ⚠ (Pt).

vibration frequencies around 3670, 3380 and 2850 cm^{-1} due to free OH, hydrogen bonded OH (of the normal OH···O variety) and hydrogen bonded OH involving Pt atoms (OH···Pt) respectively. These workers also report O···O stretching (240 cm^{-1}) and O–Pt stretching (470 cm^{-1} found only at low exposures of ~0.5 L) frequencies in addition to rotation mode frequencies of the water molecule. Molecularly adsorbed water on Pt(111) also shows peaks similar to those found in the infrared and Raman spectra of ice (Sexton, 1980). A transition between the first and second monolayers of water gives rise to a translational frequency of ~250 cm^{-1}.

Alcohols

Adsorption of methyl alcohol on Ni(111) has been studied by Demuth and Ibach (1979a) who find a methoxy species to be an intermediate during the decomposition of chemisorbed methanol. Chemisorbed CH_3OH shows bands at 3200 (O–H stretching), 2950 and 2800 (CH_3 stretching), 1455 (O–H bend), 1035 (C–O stretching), and 680 cm^{-1} (Ni–O stretching). Characteristic peaks due to methoxy species with the oxygen end nearest to the surface and the CH_3 group inclined at an oblique angle have also been assigned (Demuth and Ibach, 1979b). Sexton (1979b) finds that both CH_3OH and C_2H_5OH react with atomic oxygen on Cu(100) giving rise to alkoxy species bonded to the metal. The characteristic frequencies of CH_3O–Cu are 2910 and 2830 (CH_3 stretching), 1960 (overtone of C–O stretching), 1450 (CH_3 bend), 1010 (C–O stretching) and 290 cm^{-1} (Cu–O stretching). Similar peaks are also seen in the case of C_2H_5O–Cu except that there are additional bands at 870 (C–C stretching) and 470 cm^{-1} (O–C–C bend).

Formic acid

Decomposition of HCOOH on Cu(100) gives rise to formate ion bound to the surface in a bidentate structure (Sexton, 1979c). The peak assignments are: 2910 and 2840 (C–H stretching), 1640 (CO_2 asymmetric stretching), 1360 (symmetric CO_2 stretching), 790 (O–C–O bend) and 340 cm^{-1} (Cu–O stretching).

Co-adsorbed molecules

There have been a few studies of co-adsorbed molecules by energy loss spectroscopy. Froitzheim, Ibach and Lehwald (1977) studied co-adsorption of CO and O_2 on W(100) and found oxygen to displace α–CO. Thomas and Weinberg (1979a) have discussed co-adsorption of CO and O_2 on Ru(001) in terms of inter-adsorbate interaction and indirect through-bond interactions. In a study of the co-adsorption of CO and H_2 on W(100), β–CO is found to displace peaks due to adsorbed hydrogen; hydrogen does not adsorb on CO covered surfaces. Co-adsorption of H_2 and CO on Ni(111) surface has been investigated by Bertolini and Dalmai-Imelik (1979) who find three surface species when the surface is maintained at 410 K and then cooled to room temperature. The three species are: (a) a weakly bonded CO thermally desorbed, (b) an oxyhydrocarbonated compound and (c) a hydrocarbonated species. Surface carbide formed due to the disproportionation of CO at 410 K is expected to play a role in the formation of these species. Some of the species described are, –C(H)OH, –C(O)H and H–CO_2. Ibach and Somorjai (1979) find that co-adsorption of CO with hydrocarbons on Ni(111) and Pt(111) surfaces causes a weakening of the C–O bond as indicated by the lowering of the C–O stretching frequencies. Co-adsorption of CO and NO has also been studied recently; CO competes directly with one of the sites of NO for adsorption (Thiel, Weinberg and Yates, 1979b).

ELECTRONIC TRANSITIONS

Unlike vibrational spectra which were examined adsorbate by adsorbate, we shall review electronic transitions adsorbent by adsorbent. This is primarily because of the need to refer to the characteristic transitions of the solid adsorbent while discussing interactions with different adsorbates.

Silicon

Clean Si shows energy loss peaks due to interband transitions (E_1, E_2) around 3.5 and 4.8 eV, due to transitions involving surface states (S_1, S_2, S_3) around 2.0, 7.5 and 14.5 eV and due to surface and bulk plasmons ($\hbar\omega_s$, $\hbar\omega_p$) around 10.7 and 17 eV respectively (Ibach and Rowe, 1974a; Chung, Siekhaus and Somorjai, 1976; Fujiwara, Ogata and Nishijima, 1977; Fujiwara and Ogata, 1977). The surface state transition around 2 eV involves dangling bonds. On interaction with molecules several changes are generally noticed which include disappearance or attenuation of S_1, S_2 and S_3 peaks, appearance of new losses due to formation of bonds with Si, changes in plasmon peaks, appearance of peaks due to associatively or dissociatively adsorbed molecules and so on. In *Table 8* we have summarized the results on the interaction of various molecules on Si surfaces.

Ibach and Rowe (1974a) find that interaction of hydrogen with ordered Si surfaces causes disappearance of the surface state peaks S_1, S_2 and S_3 accompanied by a loss around 8 eV due to the formation of the Si–H bond making use of the S_1 dangling bonds. Oxygen adsorbed on Si surfaces at 300 K does not immediately give rise to an oxide layer of SiO_2 type; it is adsorbed molecularly with electronic transitions around 3.5, 7.2 and 11 eV, both on (111) and (100) surfaces (Rowe and Ibach, 1973; Ibach and Rowe, 1974b and c; Rowe, Ibach and Froitzheim, 1975). High exposures to oxygen or electron irradiation converts the adsorbed oxygen to SiO_2. Energy loss spectra have been partly interpreted based on dielectric theory by these workers but this does not agree with the earlier ideas (Steinrisser and Sickafus, 1971; Sickafus and Steinrisser, 1972; Küppers, 1973). A consequence of the dielectric model would be that the observed energy losses are not exactly equal to the energy differences between the occupied and unoccupied energy levels. EELS as well as other studies by Ibach and Rowe (1974b and c) suggest that the adsorbed oxygen is likely to form a peroxide bridge connecting the nearest neighbour atoms as earlier found from the vibrational features in high resolution electron energy loss spectra (Ibach *et al.*, 1973).

The optically forbidden $1\Sigma - 3\Pi$ transition of oxygen around 3.2 eV has been noticed on Si(100) and (111) surfaces (at low primary voltages) by Ludeke and Koma (1975). These workers have proposed that surface oxygen atoms are doubly bonded to Si and have suggested reinterpretation of the peroxide model of Ibach *et al.* (1973). The Si–O bond appears to be stronger on a disordered Si(111) surface than on an ordered Si(111) 7 × 7 surface (Chung, Siekhaus and Somorjai, 1976). The relative positions of the loss peaks are different in disordered and ordered surfaces. While the 8.4 and 7 eV peaks are both well developed on a disordered surface, only the 7.3 eV peak is strong (8.4 eV being a shoulder) on ordered surfaces. The S_1 peak is removed on the disordered surface but is still present on the ordered surface. Fujiwara, Ogata and Nishijima (1977) have assigned loss peaks to molecular as well as atomic oxygen states (but not SiO_2) on Si(111). It may be noted, however, that the positions of many of the loss peaks (3.2, 4.9, 7.1 eV) are very close to the loss peaks of clean Si surface. Adsorption of oxygen on amorphous Si results in the disappearance of the $\hbar\omega_s$ peak accompanied by some new losses (Derrien *et al.*, 1978).

TABLE 8. Electronic transitions involving molecules adsorbed on Si, Ge and Sn

Surface	Ep (eV)	Temperature (K)	Exposure	Observed electronic losses (eV)	Reference
SILICON					
Si(111) (111) 2 × 1, (111) 7 × 7	80–100	300	Clean	1.7–2 (S_1), 3.2–3.5 (E_1), 4.8–5 (E_2), 7.3–8 (S_2), 10.4–11 ($\hbar\omega_s$), 14–15 (S_3), 17–17.2 ($\hbar\omega_p$)	Ibach and Rowe, 1974a; Chung, Siekhaus and Somorjai, 1976: Fujiwara, Ogata and Nishijima, 1977; Fujiwara and Ogata, 1977
Si(100) 2 × 1	63	300		1.8 (S_1), 3.2 (E_1), 4.6 (E_2), 6.6 (S_2), 10.5 ($\hbar\omega_s$) 14.8 (S_3), 17.2 ($\hbar\omega_p$)	Miyamura *et al.*, 1978
Hydrogen					
Si(111) 2 × 1	100	300	900 L	S_1, S_2 and S_3 disappear, new loss at 7.6 (Si–H bond formed using Si dangling bonds)	Ibach and Rowe, 1974a
Si(111) 7 × 7			600–1800 L	New loss shifts to 7.9–8.3	
Si(100) 2 × 1			60–1800 L	New loss shifts to 7.5–8.5	
Oxygen					
Si(111) ordered	100	300	$\frac{1}{4}$ monolayer	S_1 and S_3 decrease in intensity, apparent increase in S_2 intensity due to oxygen induced transition, surface plasmon peak appears to split due to presence of oxygen transition at 11 eV	Rowe and Ibach, 1973; Ibach and Rowe, 1974a and b
			Up to one monolayer	New loss at 7.4	Rowe, Ibach and Froitzheim, 1975
			>One monolayer	7.4 loss decreases in intensity and a new loss at 10.7 develops	
Si(100) ordered	100	300	$\frac{1}{4}$ monolayer	S_1 disappears and losses around 7.4 and 11 due to oxygen electronic levels. SiO_2 losses are at 10.7, 12.5, 14.5, 17.8 and 28	Ibach and Rowe, 1974a and b
Si(111) Si(100)	20–100	300	Monolayer	2.9–3.4 ($1\Sigma \longrightarrow 3\pi$ optically forbidden as in gas phase); 4.8 and 6.9 (oxygen induced transitions); 8.3 and 9.4 (monoxide like bound state)	Ludeke and Koma, 1975
Si(111) disordered	100	300	$\theta = 1$	3.4, 4.9, 7, 8.3, 9.5 (all losses assigned as above) and a loss at 12.8 (oxygen induced loss)	Chung, Siekhaus and Somorjai, 1976
Si(111) (111) 7 × 7	80	300	1.2 L	3.4 (O^I_1), 4.9 (O^I_2), 7.1 (O^I_3), 9.6 ($\hbar\omega_s$), 13.2 (O^I_4), 17.9 ($\hbar\omega_p$), 20.6 (O^I_5)	Fujiwara, Ogata and Nishijima, 1977; Fujiwara and Ogata, 1977
		970	100 L	3.4 (O^{II}_1), 4.9 (O^{II}_2), 7.1 (O^{II}_3), 8.6 (O^{II}_4), 10.1 (O^{II}_5), 13.2 (O^{II}_6), 17.8 ($\hbar\omega_p$), 20.7 (O^{II}_7)	

Amorphous Si	200	300	$\theta = 1$	$\hbar\omega_s$ disappears, new losses at 7.6 (oxygen induced, light sensitive), 10.1 (E) and 12.9 (oxygen induced, light sensitive)	Derrien *et al.*, 1978
Nitric oxide					
Si(111)	100	300	θ_{sat}	New losses at 3.4 and 5.0 also at 6.9, 12.9 and 23	Nishijima and Fujiwara, 1977
		770	θ_{sat}	losses at 5 and 6.9 increase in intensity and a hump appears at 8.5	
Hydrogen halides					
Si(111)	63	300	5 L HCl 0 time	S_1, S_2, S_3, E_1 and E_2 attenuated, new loss at 8.4 (intensity decreases with time)	Miyamura *et al.*, 1978
			After 80 min	New loss at 7.0 (Si–Cl) and loss at 8.4 (Si–H) decreases	
		800		7.0 (π) increases and new losses appear at 6.0 (π) and 9.0 (σ) (all due to stable Si–Cl bond formation)	
		300	HBr exposed	Loss at 7.8 decreasing in intensity with time; no new losses seen	
Water					
Si(111)	30–200	300	10–100 L	New losses at 3.7, 7, 8.7 (extrinsic surface state transitions of H_2O), intrinsic surface state transitions diminish	Fujiwara and Nishijima, 1975; Fujiwara, Ogata and Nishijima, 1977
		970	60 L	New loss at 10.1 with a shoulder at 8.6 (surface with atomic oxygen)	Fujiwara and Ogata, 1977 and 1979
Hydrogen sulphide					
Si(111) 7 × 7	80	300	Up to 2000 L	S_1, S_2, S_3 intensity decrease, new losses at 3.7, 4.8 and 8.8 (extrinsic surface state transitions of H_2S), 10.3 ($\hbar\omega_s$), 17.8 ($\hbar\omega_p$)	Fujiwara, Ogata and Nishijima, 1977; Fujiwara and Ogata, 1978
		820	50 L	New losses at 3.4, 5.0, 7.2 (metastable SiS_x formation); 8.9, 10.3, 13.5, 18.1 ($\hbar\omega_p$), 21 (all other losses due to dissociated species)	
Ammonia					
Si(111)	50	300	θ_{sat}	New losses at 4.2, 8.7 (due to molecular species)	Nishijima and Fujiwara, 1977
		770		peak at 6.9 (nitrogen atoms)	
		1470	8×10^3 L	3.7 and 7.2 (presence of SiN_x); 10.6–20 (electronic transitions of Si_3N_4)	

TABLE 8 continued

Surface	Ep (eV)	Temperature (K)	Exposure	Observed electronic losses (eV)	Reference
Acetylene					
Si(111) 7 × 7 ordered	100	300	$\theta = 1$	New losses at 3.6 (acetylene related), 7.3, 8.4 (splitting of C_2H_2–orbitals by Si crystal field) and S_1 is still present	Chung, Siekhaus and Somorjai, 1976
(111) disordered			$\theta = 1$	3.6 and 8.4 appear and a shoulder at 7 present, S_1 is completely removed	
GERMANIUM					
Ge(100) 2 × 1, (111) 8 × 8	50–100	300	Clean	1.2 (bb to ss), 2.5 (Vb to Cb), 4.5 (Vb to Cb), 7.3 (bb to ss), 8.9 (bb to ss), 11 ($\hbar\omega_s$), 13.5 (bb to ss), 16.3 ($\hbar\omega_p$), 28.9 (d core to ss); 29.5 (d core to ss) and losses at 30.8, 32.9, 34.3 (d core to Cb) (ss, surface state dangling bond; bb, surface state back bond; Vb, valence band; Cb, conduction band)	Ludeke and Koma, 1975; Ludeke and Koma, 1976
Oxygen					
Ge(100) 2 × 1 (111) 8 × 8	100	300	$\theta = 1$	New loss at 3.4 ($a^3\Sigma^+ \rightarrow X^1\Sigma^+$), new loss at 4.5 shifting to 4.7 with coverage	Ludeke and Koma, 1975
			$\theta = 0.3$–1	ss disappears and new losses at 4.7, 6.7–6.8, 30.4 and 31.0	Ludeke and Koma, 1976
TIN					
Polycrystalline	200–1000	300	Clean	4.8 (interband $\Gamma_5^+ \rightarrow \Gamma_4^-$) 10 ($\hbar\omega_s$), 14 ($\hbar\omega_p$), 27 ($2\hbar\omega_p$) and 42 ($3\hbar\omega_p$)	Bayat-Mokhtari, Barlow and Gallon, 1979; Powell, 1979a and b
Oxygen	300	300	5×10^3 L	New losses at 9.5, 13.5 and 28 (SnO_2 loss peaks at 13.5 and 19.5, intensity of SnO loss peaks small)	
		500	Very high L	Losses at 6.2, 11.8, 17.3, 18.7 and 33	Bayat-Mokhtari, Barlow and Gallon, 1979

Nitric oxide seems to show molecular transitions at 3.4, 5.0, 6.9, 12.3 and 23 eV on a Si(111) surface at 300 K (Nishijima and Fujiwara, 1977). At 770 K, however, losses are seen similar to those with a surface covered with nitrogen and oxygen atoms; further heating to 1170–1270 K, results in a surface covered with only nitrogen atoms.

Adsorption of HCl on a Si(111) surface at 300 K has been examined by Miyamura *et al.* (1978) who notice attenuation of S_1, S_2, S_3, E_1 and E_2 peaks and a peak around 8.4 eV due to the lone pair electron of Cl (of molecularly adsorbed HCl). With time, the 8.4 eV peak intensity decreases and a loss due to Si–Cl bonds is seen around 7 eV. At 800 K, bands due to a Cl–π bonding states are seen at 6 and 7 eV and due to a σ-like state at 9 eV. Adsorption of HBr gives a lone pair peak at 7.8 eV, but distinct losses due to new (Si–Br) species have not been observed (Miyamura *et al.*, 1978).

Interaction of H_2O with Si(111) at 300 K gives extrinsic surface state transitions due to molecular water (Fujiwara and Nishijima, 1975; Fujiwara, Ogata and Nishijima, 1977; Fujiwara and Ogata, 1977). With increase in annealing temperature, the interaction seems to proceed in three steps *viz.*, molecular adsorption, dissociation and hydrogen/oxygen desorption (Fujiwara and Ogata, 1979). At high temperatures, H_2S adsorption on Si(111) results in metastable SiS_x formation while at 300 K, intensities of S_1, S_2 and S_3 diminish with the appearance of new losses due to molecularly adsorbed species (Fujiwara, Ogata and Nishijima, 1977; Fujiwara and Ogata, 1978). Ammonia similarly shows molecular adsorption at 300 K and formation of nitrides at high temperatures (Nishijima and Fujiwara, 1977). Interaction of acetylene on an ordered Si(111) 7 × 7 surface shows evidence for molecularly adsorbed C_2H_2 on a B_2 site at 300 K; this appears to result from the overlap between Si surface dangling bond orbitals and the π orbitals of C_2H_2 (Chung, Siekhaus and Somorjai, 1976). The loss peak due to S_1 still persists on the ordered surface; on the disordered surface, however, S_1 is completely removed.

Germanium

Electron states of clean Ge are shown in *Table 8*. Oxygen is adsorbed on two different sites of Ge, the more active sites being those associated with dangling bonds (Ludeke and Koma, 1976). Oxygen appears to chemisorb to form quasimolecular GeO complexes independent of surface orientation.

Tin

Loss peaks of clean Sn surface are shown in *Table 8*; the 4.7 eV peak could, however, be due to a surface oxide layer present below detection limits (Bayat-Mokhtari, Barlow and Gallon, 1979). At high exposures to oxygen, spectra of polycrystalline Sn show the presence of a mixture of Sn and SnO (in the proportion 3:2) (Powell, 1979a). EELS of fully oxidized Sn has also been reported (Bayat-Mokhtari, Barlow and Gallon, 1979; Powell, 1979b).

Nickel

Energy loss spectra of clean Ni shows interband transitions as well as surface and bulk plasmon peaks as shown in *Table 9*. *Table 9* also lists EELS data on adsorbed molecules on nickel surfaces. Adsorption of hydrogen on Ni(100), (110) or (111) surfaces gives rise to a loss around 15 eV as reported by Christmann *et al.* (1974) and the peak at 7.5 eV reported earlier by Küppers (1973) appears to arise from CO impurity. The 15 eV peak is considered to arise from the excitation of an electron from a filled chemisorption level to a higher unfilled state. Steinrisser and Sickafus (1971) and Sickafus and Steinrisser (1972)

TABLE 9. Electronic transitions involving molecules adsorbed on Ni

Surface	Ep (eV)	Temperature (K)	Exposure	Observed electronic losses (eV)	Reference
Nickel					
Ni(100), (110) and (111)	62	300	Clean	8 ($\hbar\omega_s$), 18 ($\hbar\omega_p$), 26 ($\hbar\omega_s + \hbar\omega_p$)	Küppers, 1973
Ni(100)	100	300	Clean	3.3 and 6.0 (transitions from 3 d), 9.1 ($\hbar\omega_p$ of 4s), 14 ($\hbar\omega_s$), 19 ($\hbar\omega_p$) of coupled 3 d + 4 s), 27 (3 d to higher lying p states), 33 (localized many body effect), 38 and 50 (multiple plasmon losses)	Akimoto *et al.*, 1979a Sakisaka *et al.*, 1979
Ni(110)	150	300	Clean	4.1 (E), 7.2 ($\hbar\omega_s$), 10 (E), 19.2, 26.9, 32.4, 38.3 and 65.9 (M_{23})	Benndorf *et al.*, 1979
	250	300		3.7, 8.2, 19.3, 27.2, 66.0, 110.2 (M_1)	
Hydrogen					
Ni(100), (111) and (110)	62	300	Exposed to H_2	Additional loss at 15	Küppers, 1973; Christmann *et al.*, 1974
Nitrogen					
Ni(110)	60–80	300	Disordered adlayer	New losses at 4.5 and 11.2	Steinrisser and Sickafus, 1971; Sickafus and Steinrisser, 1972

Oxygen					
Ni(100)	90–150	300	$\frac{1}{4}$ monolayer p(2 × 2)	New loss at 5.8	Murata, Ohtani and Terada, 1974
			$\frac{1}{2}$ monolayer c(2 × 2)	Above loss splits into peaks at 5.4 and 6.4	Ohtani, Terada and Murata, 1974
	40	300	$\leqslant$4 L	New losses at 6, 8 and 10.3	Akimoto *et al.*, 1979a
			>50 L	Spectra similar to NiO(100)	Sakisaka *et al.*, 1979
Ni(110)	150	300	22 L	7.2 loss vanishes and a new loss at 23.9	Benndorf *et al.*, 1979
			7×10^5 L	New losses at 5.8 and 7.4, 13.9 and 23.9; splitting of M_{23} peak	Benndorf *et al.*, 1980
Sulpur					
Ni(110)	60–80	493	c(2 × 2) S	New losses at 5.8, 7, 8.8, 11.2 and 14.2. Fitted into an energy level diagram with two occupied states below Fermi level and three unoccupied states between Fermi level and vacuum zero	Steinrisser and Sickafus, 1971; Sickafus and Steinrisser, 1972
Carbon monoxide					
Ni(110)	30–65	300	1 L	New loss at 15 shifting to 13 with increase in exposure	Küppers, 1972 and 1973
		470–670		15 loss remains; additional loss at 5.5 (presence of dissociated species)	
Ni(100)	60	300	Up to 5 L	5.8, 8.6, 11.8, 12.6 and 16.4	Akimoto *et al.*, 1979b; Sakisaka *et al.*, 1979
Ni(111)	250	300	Exposed to CO	New losses at 6.5 and 14	Rubloff and Freeouf, 1978
Nitric oxide					
Ni(110)	*100*	*300*	*0.8–100 L*	Losses at 4.8, *10.2, 12.0, 15.2*	Sakisaka *et al.*, 1980

TABLE 10. Electronic transition involving molecules adsorbed on Pt and Pd

Surface	Ep (eV)	Temperature (K)	Exposure	Observed electronic losses (eV)	Reference
PLATINUM					
Pt(111), (100) (997) and Pt[6(111) × ($\bar{1}$00)]	70–200	300	Clean	5.2, 6.5, 11.7–12 (interband transitions), 22.2–24 ($\hbar\omega_s$), 30–33 ($\hbar\omega_p$), 57 (multiple excitations)	Christmann, Ertl and Pignet, 1976; Maire, Legare and Lindauer, 1979
Polycrystalline	100	300	Clean	3.4, 6.2, 9.7 (interband transitions)	Farrell and Strauss, 1977
Hydrogen					
Pt(997), (111)	200	300	$\theta = 1$	New loss at 15–15.5 [metal *d*-band to empty hydrogen (2*s*)]	Christmann, Ertl and Pignet, 1976; Christmann and Ertl, 1976
Oxygen					
Pt[6(111) × ($\bar{1}$00)]	200	300	Low θ	New loss at 15.5 (interband) and decrease in intensity of 12	Maire, Legare and Lindauer, 1979
		873	High θ	15.5 shifts to 14.5	
Carbon monoxide					
Pt(100)	70	300	θ_{sat}	New losses at 6 [just below E_f to CO($2\pi^*$)] and 14 [intramolecular $5\sigma - 1\pi \rightarrow 2\pi^*$ of CO]	Netzer, Wille and Matthew, 1977
Pt(111)	64	300	θ_{sat}	New losses at 6 and 14	Netzer and Matthew, 1979a
	106	300	θ_{sat}	6 decreases in intensity, 14 becomes prominent	
	200	300	θ_{sat}	Losses only at 7.5 and 14 and loss at 6 vanishes	

Hydrocarbons					
Acetylene					
Pt(111)	100	300	Low θ	New losses at 4.5 and 8	Netzer and Matthew, 1979b
Ethylene					
Pt(111)	100	300	Low θ	Sharp new losses at 7.5 and 20 with a shoulder at 14	
		170	Low θ	Absence of 7.5 loss	
Benzene					
Pt(111)	100	300	Low θ	Considerable loss structure around 25 and absence of 7.5 loss	
Cyanogen					
Pt(100)	70	300	11.5 L	New losses at 11 and 14	Wille, Netzer and Matthew, 1977
PALLADIUM					
Pd(111), (001), [(001] 6°(110)]	200	300	Clean	7, 14 and 16 (interband transitions), 24 ($\hbar\omega_s$), 32 ($\hbar\omega_p$), 44 (combined loss)	Bader *et al.*, 1978; Legare, Holl and Maire, 1979
Oxygen					
Pd(111)	200	300	60 L	New loss at 18 and 14 loss peak sensitive to oxygen adsorption	Legare, Holl and Maire, 1979
Carbon monoxide					
Pd(001) and [(001) 6°(110)]	75	300	Low θ	New loss at 13.5 and absence of 6–7 loss (d–π^*)	Bader *et al.*, 1978

have observed that a disordered adlayer of nitrogen on Ni(110) gives rise to a loss at 4.5 eV due to a transition from the *d*-band to a bound excited state 3.5 eV above the Fermi level. A loss peak is found at 11.2 eV due to a transition from a low-lying molecular orbital to an excited state level above E_f.

Akimoto *et al.* (1979a) have reported that adsorption of oxygen on Ni(100) gives rise to bands at 6.8 and 10.3 eV at $\leqslant$4L exposure due to the charge-transfer transitions: $O(2p)_e \rightarrow Ni(3d)$, $O(2p)_a \rightarrow Ni(3d)$ and $O(2p) \rightarrow Ni(4s)$ respectively. Above 50 L exposure, the losses are similar to NiO(100). Ohtani, Terada and Murata (1974) and Murata, Ohtani and Terada (1974) find a loss peak at 5.8 eV when $\frac{1}{4}$ monolayer of oxygen is adsorbed on Ni(100) due to the excitation of electrons in the Ni–O bond; this loss peak splits into two peaks at 5.4 and 6.4 eV at half coverage due to the formation of different types of species. Benndorff *et al.* (1979 and 1980) report loss peaks at 5.8, 7.4, 13.9 and 23.9 eV at high oxygen exposures on a Ni(100) surface and this is accompanied by the splitting of M_{23} loss peak around 66 eV. The 5.8 and 7.4 eV losses are assigned to excitations arising from O(2*p*) to unfilled levels near the Fermi level. While the 13.9 eV loss is assigned to combined $2p \rightarrow 4s$, $2p \rightarrow 3d^9$ and $2p \rightarrow 3d^7 + 3d^9$ transitions, the 23.9 eV loss is due to excitation from O(2*s*).

Rubloff and Freeouf (1978) have reported a loss peak at 6.5 eV due to the $Ni(3d) \rightarrow CO(2\pi^*)$ charge-transfer transition when CO is adsorbed on Ni(111). They also find a peak at 14 eV which they assign to a Rydberg transition. Akimoto *et al.* (1979b) find that adsorption of carbon monoxide on Ni(100) gives rise to $Nid\pi \rightarrow CO(2\pi^*)$ and $Nid\sigma \rightarrow CO(2\pi^*)$ charge-transfer bands at 5.8 and 8.6 eV respectively and intramolecular transitions $5\sigma \rightarrow 2\pi^*$, $1\pi \rightarrow 2\pi^*$ and $4\sigma \rightarrow 2\pi^*$ at 11.8, 12.6 and 16.4 eV respectively, the 12.6 eV peak being sensitive to CO–CO interaction (shifts to 13.7 eV with increase in exposure). Küppers (1972) had earlier found a loss peak at 15 eV which shifts to 13 eV with increase in exposure to CO on Ni(110) at 300 K. With increase in temperature, evidence was found for the dissociation of CO.

Sakisaka *et al.* (1980) find that nitric oxide is dissociatively adsorbed below 0.8 L exposure. Between 0.8 and 100 L there is coexistence of molecular NO with losses at 4.8, 10.2, 12.0 and 15.2 eV.

Platinum

Energy loss peaks from Pt surfaces are shown in *Table 10.* Adsorption of H_2 gives rise to a new loss peak at 15 eV which has been assigned to a transition from the metal *d*-band to empty hydrogen (2*s*) level (Christmann, Ertl and Pignet, 1976). Adsorption of oxygen gives rise to a new loss at 15.5 eV accompanied by a decrease in the intensity of the 12 eV interband transition (Maire, Legare and Lindauer, 1979). At high exposures, the 15.5 eV loss peak is shifted to 14.5 eV.

Adsorption of CO on platinum gives rise to two new losses at 6 and 14 eV. The 6 eV loss is due to a charge-transfer transition from the metal *d*-band to adsorbed $CO(2\pi^*)$ level and this transition is also seen when CO is adsorbed on Cu and Ni. The 14 eV loss is generally seen in most metals and these losses have been listed by Bader *et al.* (1978). Netzer, Wille and Matthew (1977) assign the 14 eV loss to an intramolecular transition of $CO(5\sigma\text{–}1\pi) \rightarrow CO(2\pi^*)$. These two losses of adsorbed CO seem to be affected by a decrease in the energy difference between the 5σ and 1π levels and by the large upward shifts in the excited $2\pi^*$ level (as in the case of metal carbonyls). The final state of the 14 eV loss has been considered to involve excited states involving $2\pi^*$ molecular orbitals as well as unfilled metal orbitals (Netzer and Matthew, 1979a).

Adsorption of acetylene on polycrystalline Pt gives rise to new losses at 4.5 and 8 eV, the first arising from a $d\pi$ level and the second from the C–H σ bond; both the π and π^*

orbitals of C_2H_2 seem to be involved in chemisorption (Farrell and Strauss, 1977). Adsorption of C_2H_4 at room temperature gives rise to sharp losses at 7.5 and 20 eV and a shoulder at 14 eV (Netzer and Matthew, 1979b). The 7.5 eV loss peak has been assigned to the vinyl species formed around room temperature; this peak disappears at 170 K suggesting rehybridization to an sp^3 type configuration at low temperature. It may be recalled (*see* acetylene section) that Ibach and Lehwald (1978a) have proposed an ethylidene ($>CH{-}CH_3$) species while Kesmodel, Dubois and Somorjai (1978) have proposed an ethylidyne ($\geqslant C{-}CH_3$) species to describe ethylene adsorbed on Pt(111).

Benzene adsorbed on Pt(111) does not show a loss peak around 7.5 eV suggesting that the π–π^* transition is inhibited (Netzer and Matthew, 1979b). A broad 25 eV loss is observed, but the origin of this is not clear. A 7 eV electron loss peak due to a π–π^* transition of pyridine adsorbed on Ir(111) has been found but the same transition in benzene is very weak, both benzene and pyridine show weak losses (4–5 eV) due to d–π^* charge-transfer transitions (Netzer, Bertel and Matthew, 1980).

Cyanogen adsorbed on Pt(100) gives new losses around 11 and 14 eV indicating an upward shift of the $2\pi^*$ state due to mixing with metal orbitals (Willie, Netzer and Matthew, 1977). There appears to be some doubt as to whether cyanogen adsorbs molecularly or as CN species.

Palladium

It has been shown that the 14 eV interband transition of Pd(111) is sensitive to oxygen adsorption (Legare, Holl and Maire, 1979). Adsorption of oxygen also gives rise to a loss around 18 eV due to a transition from O(2p) to a metal level 12 eV above the Fermi level. Adsorption of CO on Pd(001) gives rise to a new loss at 13.5 eV due to 5σ–$1\pi \rightarrow 2\pi^*$ transition of adsorbed CO; the 6–7 eV charge-transfer transition is not seen on this surface (Bader *et al.*, 1978). EELS data on molecules adsorbed on Pd surfaces are given in *Table 10.*

Tungsten

The loss peaks due to clean tungsten surfaces are shown in *Table 11* along with those due to adsorbed molecules. Avery (1976) has reported that adsorption of oxygen causes attenuation of the loss peaks at 2.7 and 5.2 eV. Increase in exposure up to 0.67 L gives rise to new losses at 3.4 and 8 eV, the latter shifting monotonically to 7.5 eV at 6.7 L. Luscher (1977) and Luscher and Propst (1977) find a loss at 7.7 eV when $\theta = 0.5$ which they assign to an O(2p) → metal d-band transition; an additional loss at 12.7 eV occurring at $\theta > 0.5$ has been assigned to an O(2s) → metal d-band transition. These workers also notice changes in the surface and bulk plasmon features at 21 and 25.5 eV respectively. Codeposition of Cs and O_2 on W(110) gives rise to losses at 10 and 15 eV associated with Cs (5p) and a loss at 26 eV associated with Cs(5s) levels; growth of thick Cs–O layers gives losses at 4.8 and 7.8 eV associated with the O(2p) level (Papageorgopoulous and Desplat, 1980).

Adsorption of CO, H_2 and I_2 on W(100) surfaces are found to give rise to losses at 7.5, 7.7 and 8.5 eV respectively (Avery, 1976). The last two losses are weak, but clearly resolved at 8 and 100 L respectively. Attenuation of the 2.7 and 5 eV losses was also noticed, the peaks being finally replaced by a broad new loss at 3.4 eV. According to Chesters, Hopkins and Winton (1976), associative adsorption of CO on W(100) gives rise to loss peaks at 5.3 and 14 eV. We assign the 14 eV peak to 5σ–$1\pi \rightarrow 2\pi^*$ transition of adsorbed CO and the 5.3 eV peak to the metal $d \rightarrow$ CO($2\pi^*$) charge-transfer transition. Adsorption of nitrogen on W(100) shows losses due to both α and β

TABLE 11. Electronic transitions involving molecules adsorbed on W and Mo

Surface	Ep (eV)	Temperature (K)	Exposure	Observed electronic losses (eV)	Reference
TUNGSTEN W(100)	25–115	300	Clean	2–2.7, 4.5, 4.6, 10.7–10.9, 12, 14.6, 17 (inter and intraband transitions involving both valence and conduction bands), 21 ($\hbar\omega_s$) and 25.5 ($\hbar\omega_p$)	Luscher, 1977; Luscher and Propst, 1977; Rawlings, Hopkins and Foulias, 1978
Oxygen W(100)	25–115	300	$\theta = 0.5$	New loss at 7.7	Luscher, 1977; Luscher and Propst, 1977; Avery, 1976
			$\theta > 0.5$	Another loss at 12.7	
			0.67–6.7 L	Losses at 3.4 and 7.5–8 (interband transitions)	
Carbon monoxide W(100)	25	300	Low θ	Losses at 5.3, 9.1 (shoulder), 14	Chesters, Hopkins and Winton, 1976
Nitrogen W(100)	70	300	θ_{sat}	Losses at 10 (β state) and 4.2, 9.6 (weak), 15.1 (α state)	Chesters, Hopkins and Winton, 1976
Acetylene W(100)	60	300	Submonolayer	New losses at 4.4 and 7 (molecular) 4.4 disappears on heating	Rawlings, Hopkins and Foulias, 1978
MOLYBDENUM Mo foils, Mo(100)	70–300	300	Clean	2.4 (bulk interband), 3.1, 4.2 and 4.9–5.1 (ss transitions), 7.2 (bulk interband), 9.5–10 ($\hbar\omega_s$), 10.5–10.6 (E) 15.6 ($\hbar\omega_s + 4.9$), 21.5–23 ($\hbar\omega_p$), 31.8 ($4p \rightarrow E_f$), 36.4 ($4p$ to 2.2 eV above E_f)	Kawai *et al.*, 1974; Ballu, Lecante and Rousseau, 1976; Wilson, 1976
Oxygen Mo(100)	50–80	300	0.6 L	4.2 loss disappears, 7.2 loss shifts to 6.9, 9.5 loss shifts to 10.3	Kawai *et al.*, 1974
			~5 L	Broad losses at 5 and 6.9	Ballu, Lecante and Rousseau, 1976
Hydrogen sulphide Mo(100)	100	300	Low θ	4.9 (surface sensitive) decreases in intensity, 10.5 shifts to 10.2, 15.6 disappears, other losses shift to higher energies, new losses at 7.5 and 17	Wilson, 1976

states. The α state is characterized, by peaks at 4.2, 9.6 and 15.1 eV which have been respectively assigned to transitions involving $A^3\Sigma_u^-$, $a^1\Pi g$ and $2\Sigma g^+$ of the excited N_2^+ states respectively. The β state gives rise to a loss at 10 eV.

Adsorption of C_2H_2 on W(100) has been studied by Rawlings, Hopkins and Foulias (1978) who find loss peaks at 4.4 and 7 eV at submonolayer coverages. The 4.4 eV loss peak persists even at saturation but disappears on heating. At 1100 K, losses are found at 5.5, 9.5 and 13.2 eV and these are assigned to species arising from dissociation. Presaturation of the surface at 1100 K with acetylene results in a spectrum similar to the one found at saturation coverages at low temperatures with the exception of the 4.4 eV peak (Rawlings, Hopkins and Foulias, 1978).

Molybdenum

EELS data of clean Mo surface are shown in *Table 11*. On exposure to 0.6 L oxygen, the 4.2 eV surface loss disappears and the losses at 7.2 and 9.5 eV are shifted to 6.9 and 10.3 respectively (Kawai *et al.*, 1974; Ballu, Lecante and Rousseau, 1976). The 7.1 eV loss is related to the presence of first layers of oxygen atoms bonded to metal atoms and the transition may involve a state 6 eV below E_f and an empty state near E_f. The 5 eV peak found at an exposure of 5 L may arise from the (110) facets formed on the surface. Random adsorption of H_2S on Mo(100) gives rise to new features at 7.5 and 17 eV; the 7.5 eV peak has been assigned to a transition from a state 5.3 eV below E_f to one at 2.2 eV above E_f while the 17 eV loss peak is assigned to an interband transition from the (3*s*) level of sulphur (Wilson, 1976). In addition to these losses, the surface-sensitive loss peak at 4.9 eV decreases in intensity. While some of the loss peaks are shifted, the 15.6 eV peak disappears completely.

Other metals

In *Table 12* we have summarized the available information on the EELS study of the interaction of gases with surfaces of Ti, V, Cr, Cu, Ag, Au and Zn. Interaction of oxygen with Ti, V and Cr up to a coverage of $\theta = 0.4$ causes a decrease in intensity of the loss peaks around 5 and 16–17 eV, the latter disappearing completely in the case of Ti (Simmons and Scheibner, 1972). Jenkins and Chung (1971) find that interaction of oxygen with Cu(111) up to 3.5×10^3 L does not give rise to any new loss but causes only a decrease in intensity of the surface losses. Benndorf *et al.* (1978) have, however, found new losses at 5.6, 14.4 and 24.5 eV at an exposure of 10^8 L oxygen. The above three losses have been ascribed to O(2*p*) → E_f, single electron excitation involving O(2*s*) and O(2*s*) → E_f transitions respectively.

Exposure of Au(111) to 0.3 Torr oxygen (Legare *et al.*, 1980) at 620 K results in no new losses but only a decrease in intensity of the interband transitions involving surface states at 7.9 and 13 eV. Interaction of oxygen with Zn(0001) surface also gives rise to no new losses up to 60 L, but when a saturated oxide overlayer is formed, losses are seen at 4, 7, 12.7, 15 and 17 eV due to transitions from occupied surface states, O(2*p*) → conduction band, Zn(4*s*) → conduction band, $\hbar\omega_s$ and $\hbar\omega_p$ respectively (Unertl and Blakely, 1977). EELS of Cu(311), Ag(111) and Au(100) surfaces exposed to xenon has been studied (Papp, 1976; McElhiney, Papp and Pritchard, 1976; McElhiney and Pritchard, 1976). In the case of Cu(311) and Ag(111), new losses are found at 13 and 13.5 eV respectively besides two additional losses above 60 eV. The 13 eV transition is likely to involve orbitals of adsorbed Xe and the metal. In the case of Au(100), new losses are seen at 11.0, 12.3, 24, 65, 67 and 75 eV.

Interaction of carbon monoxide (Papp and Pritchard, 1975 and Papp, 1976) with

TABLE 12. Electronic transitions involving molecules adsorbed on Ti, V, Cr, Cu, Ag, Au and Zn

Surface	Ep (eV)	Temperature (K)	Exposure	Observed electronic losses (eV)	Reference
TITANIUM					
Evaporated film	100	300	Clean	5.0 ($\hbar\omega_s$), 11.5 ($\hbar\omega_p$), 17 ($\hbar\omega_s + \hbar\omega_p$), 24.0 ($2\hbar\omega_p$)	Simmons and Scheibner, 1972
Oxygen					
Evaporated Ti film	100	300	$\theta = 0.4$	Loss at 5 decreases in intensity, loss at 17 disappears	
VANADIUM					
Evaporated film	100	300	Clean	5.1 ($\hbar\omega_s$), 10.5 ($\hbar\omega_p$), 16.5 ($\hbar\omega_s + \hbar\omega_p$), 24.0 ($2\hbar\omega_p$)	Simmons and Scheibner, 1972
Oxygen					
Evaporated V film	100	300	$\theta = 0.4$	Decrease in intensity of 5.1 and 16.5	
CHROMIUM					
Evaporated film	100	300	Clean	5.0 ($\hbar\omega_s$), 9.5 ($\hbar\omega_p$), 15.5 ($\hbar\omega_s + \hbar\omega_p$), 23.5 ($2\hbar\omega_p$)	Simmons and Scheibner, 1972
Oxygen					
Evaporated Cr film	100	300	$\theta = 0.4$	Decrease in intensity of 5.0 and 15.5 losses	
COPPER					
Cu(111), (100), (311)	60–400	300	Clean	3.9–4.7 (interband transition), 7.1–7.7 ($\hbar\omega_s$), 9.7–10.5 (interband), 18.8–19.8 ($\hbar\omega_p$), 26.5, 59 and 74.5 (combined losses)	Jenkins and Chung, 1971; Papp and Pritchard, 1975; Papp, 1976; Kessler and Thieme, 1977; Benndorf *et al.*, 1978
Xenon					
Cu(311)	40–400	300	Low θ	Decrease in intensity of 4.5 and 7.7, losses and new losses at 13, 63 and 78	Papp, 1976
Oxygen					
Cu(111)	100	300–570	3.5×10^3 L	All losses of clean surface decrease in intensity, no shifts or no new losses seen	Jenkins and Chung, 1971
Cu(100)	400	400	10^3 L	New losses at 5.6, 14.4 and 24.5	Benndorf *et al.*, 1978
Carbon monoxide					
Cu(111)	150	300	6 L	Losses at 4.7, 7.7, 10 and 13.8, 10 loss disappears on flashing at 450 K	Kessler and Thieme, 1977
Cu(311)	40	77	Low θ	New losses at 4.5 and 13.5	Papp and Pritchard, 1975; Papp, 1976

SILVER					
Ag(111)	50	300	Clean	4.2 (interband), 8.2 ($\hbar\omega_p$), 12.1 (interband), 17.5 (interband or $\hbar\omega_s$ of valence electron), 25.5 (combined loss)	McElhiney, Papp and Pritchard, 1976
Xenon					
Ag(111)	40–150	300	Low θ	New losses at 13.5, 68 and 78	McElhiney, Papp and Pritchard, 1976
Carbon monoxide					
Ag(111)	50	300	Low θ	New loss at 13.5	McElhiney, Papp and Pritchard, 1976
GOLD					
Au(100)	150	300	Clean	2.5, 6.0, 9.5, 16, 20, 23 and 31 (all losses due to overlapping collective and single e$^-$ excitations), 57 (excitation from 5*p* level)	McElhiney and Pritchard, 1976
Au(111)	150	300	Clean	7, 9, 13 (interband transitions involving surface states), 24 ($\hbar\omega_s$), 33 ($\hbar\omega_p$)	Legare *et al.*, 1980
Xenon					
Au(100)	50–300	585	Low θ	New losses at 11, 12.3, 24, 65, 67 and 75	McElhiney and Pritchard, 1976
Oxygen					
Au(111)	150	620	High θ	Losses at 7, 13 and mainly at 9 decrease in intensity, losses at 24 and 33 unaffected	Legare *et al.*, 1980
Carbon monoxide					
Au(100)	150	300	Low θ	New loss at 13.5	McElhiney and Pritchard, 1976
ZINC					
Zn(0001)	60	300	Clean	8.6 ($\hbar\omega_s$), 9.4 ($\hbar\omega_p$), 10.5–11 (interband transitions involving 3 *d* band)	Unertl and Blakely, 1977
Oxygen					
Zn(0001)	60	300	60 L	No new losses seen but decrease in intensity of the clean surface losses	Unertl and Blakely, 1977
			Saturated oxide overlayer	4 (transition from occupied ss), 7 [O(2*p*) → conduction band], 12.7 [Zn(4*s*) → conduction band], 15 ($\hbar\omega_s$), 17 ($\hbar\omega_p$)	

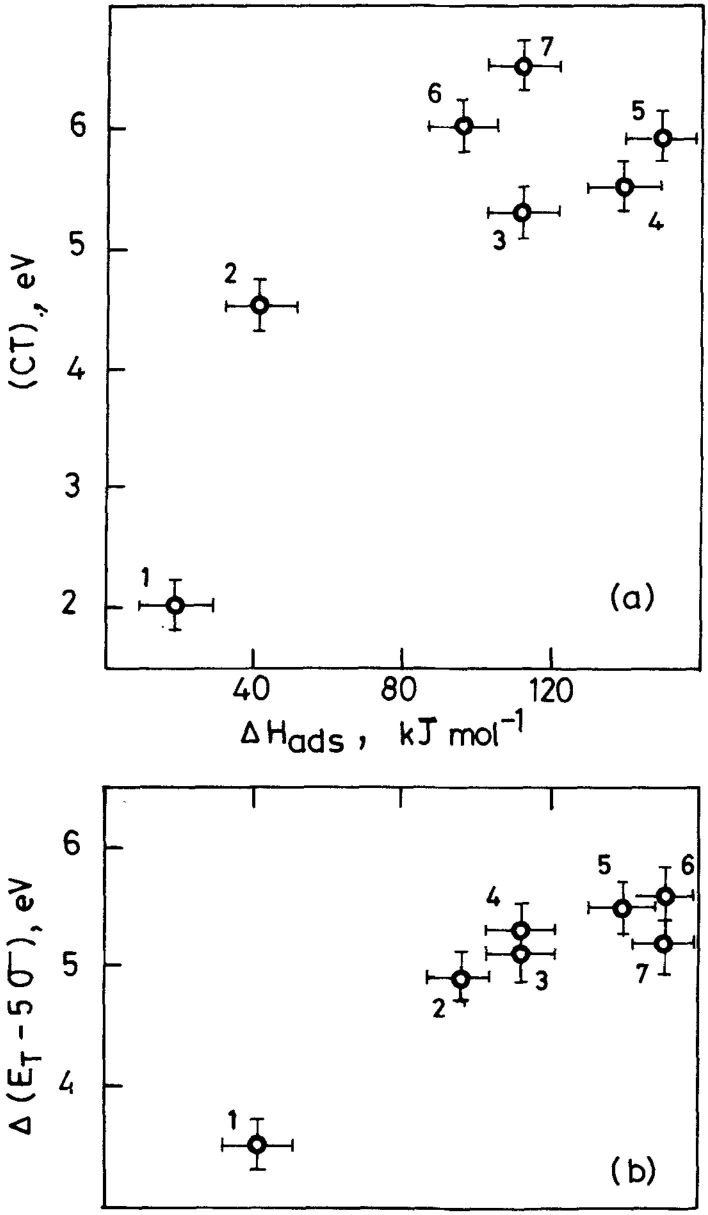

FIG. 12. (a) Plot of the metal d–π^* (CO) charge transfer energy against the heat of adsorption: 1, Ag(111); 2, Cu(311); 3, W(100); 4, Ni(110); 5, Ni(100); 6, Pt(111) and Pt(100); 7, Ni(111) (after Rao, Srinivasan and Jagannathan, 1981). (b) Plot of the π^* (CO) orbital energy against the heat of adsorption: 1, Cu(311); 2, Pt(111) and Pt(100); 3, W(100); 4, Ni(111); 5, Ni(110); 6, Pd(100); 7, Ni(100) (after Rao, Srinivasan and Jagannathan, 1981). The values for heats of adsorption are taken from Somorjai (1979).

TABLE 13. Electronic transitions involving oxygen adsorbed on Mg, Al, Te and Bi

Surface	Ep (eV)	Temperature (K)	Exposure	Observed electronic losses (eV)	Reference
MAGNESIUM Polycrystalline	750	300	Clean	7.1 ($\hbar\omega_s$), 10.6 ($\hbar\omega_p$)	Powell and Swan, 1960
Oxygen Polycrystalline Mg	750	300	Low θ Surface oxide	New loss at 4.9 (chemisorption induced transition) Losses at 22.2 and 39.4 (corresponding to bulk oxide)	
ALUMINIUM Polycrystalline	100	300	Clean	2.5 (interband), 10–10.3 ($\hbar\omega_s$), 15–15.4 ($\hbar\omega_p$), 24–25 ($\hbar\omega_s + \hbar\omega_p$), 30 ($2\hbar\omega_p$)	Simmons, 1970; Jenkins and Chung, 1971; Benndorf *et al.*, 1977
Oxygen Polycrystalline Al	100	300	Low θ Surface oxide	New loss at 7.3 (chemisorption induced transition) Loss at 22.2 (corresponding to bulk oxide) and loss at 7.3 diminished in intensity	
TELLURIUM Evaporated film	200–500	300	Clean	5.2 (interband), 11.8 ($\hbar\omega_s$), 17.0 ($\hbar\omega_p$), 33.8 ($2\hbar\omega_p$) and 41.5 ($N_{4,5}$)	Musket, 1978
Oxygen Evaporated Te film	200–500	473	Surface oxide	4.2 (interband), 12.2 ($\hbar\omega_s$), 18.5 ($\hbar\omega_p$) and 46.0 ($N_{4,5}$)	
BISMUTH Bi(0001)	30–100	300	Clean	6.5 ($\hbar\omega_s$), 14 ($\hbar\omega_p$), 24.5 ($5d_{5/2}$) 27.5 ($5d_{3/2}$)	Taylor, Rogers and Ellis, 1979
Oxygen Bi(0001)	30–100	300	10^4 L Heavily oxidized surface	9.3 ($\hbar\omega_s$), 15 ($\hbar\omega_p$), 24.5, 26.5, 28.5 Additional losses at 25.8, 27.0, 29.3 and 30.8	Taylor, Rogers and Ellis, 1979

Cu(311) surface gives rise to new losses at 4.5 and 13.5 eV due to the metal $d \rightarrow \mathrm{CO}(2\pi^*)$ charge-transfer transition and the 5σ–$1\pi \rightarrow 2\pi^*$ intramolecular transition of adsorbed CO respectively. A 13.5 eV transition is also seen in the case of Ag(111) and Au(100) surfaces exposed to carbon monoxide which is likely to be due to the intramolecular transition of adsorbed carbon monoxide.

We ourselves have data on transition metal d band $\rightarrow \mathrm{CO}(\pi^*)$ charge-transfer transition energies in the case of Cu(311), W(100), Pt(100), Pt(111), Ni(111) and Ni(110) surfaces. It is found that these transition energies bear a simple relation with the heat of adsorption of carbon monoxide on these solid surfaces (*Fig. 12a*). Knowing the binding energies of the 5σ levels of CO adsorbed on various metals from UVPS studies and the intramolecular transition energy, E_T, from EELS studies, the π^* energy, $\Delta(E_T–5\sigma)$, is plotted against the heat of adsorption in *Fig. 12b* which shows a linear relation between the two. We see that the slope of this plot is not very different from the CT transition energy *vs* ΔH_{ads} plot indicating thereby that the variation in the CT transition energy with the metal is also mainly due to the shifting of the π^* level.

In *Table 13* we have shown assorted EELS data on the interaction of oxygen with Al, Mg, Te and Bi. In all these cases losses due to surface oxide layers have been identified; losses due to chemisorbed oxygen seem to have been found only in the case of Mg and Al.

CONCLUDING REMARKS

There is little doubt that electron energy loss spectroscopy has emerged as a powerful tool for studying molecules adsorbed on surfaces. The information provided by EELS has a direct bearing on the structure and stereochemistry of the adsorbed species. Correlations of vibrational spectra from EELS with other data such as heats of adsorption, throw additional light on gas-solid interactions. Study of electronic excitations by EELS has been valuable in understanding electronic states of adsorbates and adsorbents.

Hitherto most of the studies have been limited to model systems, particularly on single crystals of metals. Such information provides the basis for understanding the behaviour of molecules adsorbed on more complex surfaces such as polycrystalline materials and metals dispersed on high surface area supports (as in catalysis). EELS studies on such complex surfaces will undoubtedly be carried out in the years to come. A limitation in the application of this technique arises from its inability to cope with catalysts under so-called ambient conditions.

Vibrational spectra of adsorbed molecules obtained by EELS and other techniques are generally comparable as they both yield insights into the nature of the bonding within the molecular fragments bound to the surface. Thus, in the case of CO adsorbed on metals, there is good agreement between results obtained from EELS and infrared spectroscopy. The situation is not, however, satisfactory in the case of C_2H_4 adsorbed on metal surfaces. There is still considerable scope for careful experimentation on model systems employing a variety of techniques including photoelectron spectroscopy, Auger spectroscopy and infrared spectroscopy.

ACKNOWLEDGEMENTS

The authors thank the Department of Science and Technology, Government of India, for support of this research in electron spectroscopy. Their thanks are due to Professors A. D. Buckingham, N. Sheppard and J. M. Thomas for their constructive suggestions and comments.

REFERENCES

AKIMOTO, K., SAKISAKA, Y., NISHIJIMA, M. and ONCHI, M. (1979a). *Surf. Sci.*, *82*, 349.

AKIMOTO, K., SAKISAKA, Y., NISHIJIMA, M. and ONCHI, M. (1979b). *Surf. Sci.*, *88*, 109.

ANDERSSON, S. (1977a). *Solid State Commn.*, *21*, 75.

ANDERSSON, S. (1977b). *Solid State Commn.*, *24*, 183.

ANDERSSON, S. (1979a). *Surf. Sci.*, *79*, 385.

ANDERSSON, S. (1979b). *Surf. Sci.*, *89*, 477.

ANDERSSON, S. and DAVENPORT, J. W. (1978). *Solid State Commn.*, *28*, 677.

AVERY, N. R. (1976). *Chem. Phys. Lett.*, *43*, 250.

BACKX, C., FEUERBACHER, B., FITTON, B. and WILLIS, R. F. (1977a). *Phys. Lett.*, *60A*, 145.

BACKX, C. and WILLIS, R. F. (1978). *Chem. Phys. Lett.*, *53*, 471.

BACKX, C., WILLIS, R. F., FEUERBACHER, B. and FITTON, B. (1977b). *Surf. Sci.*, *68*, 516.

BADER, S. D., BLAKELY, J. M., BRODSKY, M. B., FRIDDLE, R. J. and PANOSH, R. L. (1978). *Surf. Sci.*, *74*, 405.

BALLU, Y., LECANTE, J. and ROUSSEAU, H. (1976). *Phys. Rev.*, *B14*, 3201.

BARNES, M. B. and WILLIS, R. F. (1978). *Phys. Rev. Lett.*, *41*, 1729.

BARO, A. M., IBACH, H. and BRUCHMANN, H. D. (1979). *Surf. Sci.*, *88*, 384.

BARO, A. M. and IBACH, H. (1980) *Surf. Sci.*, *92*, 237.

BAYAT-MOKHTARI, P., BARLOW, S. M. and GALLON, T. E. (1979). *Surf. Sci.*, *83*, 131.

BENNDORF, C., EGERT, B., KELLER, G., SEIDEL, H. and THIEME, F. (1979). *Surf. Sci.*, *80*, 287.

BENNDORF, C., EGERT, B., KELLER, G. and THIEME, F. (1978). *Surf. Sci.*, *74*, 216.

BENNDORF, C., EGERT, B., NOBL, C., SEIDEL, H. and THIEME, F. (1980). *Surf. Sci.*, *92*, 636.

BENNDORF, C., KELLER, G., SEIDEL, H. and THIEME, F. (1977). *Surf. Sci.*, *67*, 589.

BERTOLINI, J. C. and DALMAI-IMELIK, G. (1979). *Surf. Sci.*, *80*, 586.

BERTOLINI, J. C., DALMAI-IMELIK, G. and ROUSSEAU, J. (1977a). *Surf. Sci.*, *67*, 478.

BERTOLINI, J. C., DALMAI-IMELIK, G. and ROUSSEAU, J. (1977b). *Surf. Sci.*, *68*, 539.

BERTOLINI, J. C., MASSARDIER, J. and DALMAI-IMELIK, G. (1978). *J. Chem. Soc. Faraday Trans.*, *74*, 1720.

BERTOLINI, J. C. and ROUSSEAU, J. (1979a). *Surf. Sci.*, *83*, 531.

BERTOLINI, J. C. and ROUSSEAU, J. (1979b). *Surf. Sci.*, *89*, 467.

CHESTERS, M. A., HOPKINS, B. J. and WINTON, R. I. (1976). *Surf. Sci.*, *59*, 46.

CHRISTMANN, K. and ERTL, G. (1976). *Surf. Sci.*, *60*, 365.

CHRISTMANN, K., ERTL, G. and PIGNET, T. (1976). *Surf. Sci.*, *54*, 365.

CHRISTMANN, K., SCHOBER, O., ERTL, G. and NEWMANN, M. (1974). *J. Chem. Phys.*, *60*, 4528.

CHUNG, Y. W., SIEKHAUS, W. and SOMORJAI, G. A. (1976). *Surf. Sci.*, *58*, 341.

DALMAI-IMELIK, G., BERTOLINI, J. C. and ROUSSEAU, J. (1977). *Surf. Sci.*, *63*, 67.

DAVENPORT, J. W., HO, W. and SCHRIEFFER, J. R. (1978). *Phys. Rev.*, *B17*, 3115.

DEMUTH, J. E. (1979). *Surf. Sci.*, *80*, 367.

DEMUTH, J. E. (1980). *Surf. Sci.*, *93*, L 82.

DEMUTH, J. E. and IBACH, H. (1978). *Surf. Sci.*, *78*, L 238.

DEMUTH, J. E. and IBACH, H. (1979a). *Chem. Phys. Lett.*, *60*, 395.

DEMUTH, J. E. and IBACH, H. (1979b). *Surf. Sci.*, *85*, 365.

DEMUTH, J. E., IBACH, H. and LEHWALD, S. (1978). *Phys. Rev. Lett.*, *40*, 1044.

DERRIEN, J., GOLDSTEIN, B., CROSS, A. and SALVAN, F. (1978). *Appl. Phys. Lett.*, *33*, 881.

DUBOIS, L. H., CASTNER, D. G. and SOMORJAI, G. A. (1980). *J. Chem. Phys.*, *72*, 5234.

DUBOIS, L. H. and SOMORJAI, G. A. (1979). *Surf. Sci.*, *88*, L 13.

DUBOIS, L. H. and SOMORJAI, G. A. (1980). *Surf. Sci.*, *91*, 514.

ERLEY, W., IBACH, H., LEHWALD, S. and WAGNER, H. (1979). *Surf. Sci.*, *83*, 585.

ERLEY, W., WAGNER, H. and IBACH, H. (1979). *Surf. Sci.*, *80*, 612.

ERTL, G. and KÜPPERS, J. (1974). *Low Energy Electrons and Surface Chemistry.* Verlag Chemie, Weinheim.

FARRELL, H. H. and STRAUSS, E. S. (1977). *J. Vac. Sci. and Tech.*, *14*, 427.

FROITZHEIM, H., HOPSTER, H., IBACH, H. and LEHWALD, S. (1977). *Appl. Phys.*, *13*, 147.

FROITZHEIM, H., IBACH, H. and LEHWALD, S. (1975). *Phys. Lett.*, *55A*, 247.

FROITZHEIM, H., IBACH, H. and LEHWALD, S. (1976). *Phys. Rev.*, *B14*, 1362.

FROITZHEIM, H., IBACH, H. and LEHWALD, S. (1977). *Surf. Sci.*, *63*, 56.

FUJIWARA, K. and NISHIJIMA, M. (1975). *Phys. Lett.*, *55A*, 211.

FUJIWARA, K. and OGATA, H. (1977). *J. Appl. Phys.*, *48*, 4360.

FUJIWARA, K. and OGATA, H. (1978). *Surf. Sci.*, *72*, 157.

FUJIWARA, K. and OGATA, H. (1979). *Surf. Sci.*, *86*, 700.

FUJIWARA, K., OGATA, H. and NISHIJIMA, M. (1977). *Solid State Commn.*, *21*, 895.

GLAND, J. L., SEXTON, B. A. and FISHER, G. B. (1980). *Surf. Sci.*, *95*, 587.

HO, W., WILLIS, R. F. and PLUMMER, E. W. (1978). *Phys. Rev. Lett.*, *40*, 1463.

HO, W., WILLIS, R. F. and PLUMMER, E. W. (1980). *Surf. Sci.*, *95*, 171.

HOPSTER, H. and IBACH, H. (1978). *Surf. Sci.*, *77*, 109.

IBACH, H. (1977). *Surf. Sci.*, *66*, 56.

IBACH, H. and BRUCHMANN, H. D. (1980). *Phys. Rev. Lett.*, *44*, 36.

IBACH, H., HOPSTER, H. and SEXTON, B. A. (1977). *Appl. Phys.*, *14*, 21.

IBACH, H., HORN, K., DORN, R. and LUTH, H. (1973). *Surf. Sci.*, *38*, 433.

IBACH, H. and LEHWALD, S. (1978a). *J. Vac. Sci. and Tech.*, *15*, 407.

IBACH, H. and LEHWALD, S. (1978b). *Surf. Sci.*, *76*, 1.

IBACH, H. and LEHWALD, S. (1980). *Surf. Sci.*, *91*, 187.

IBACH, H., LEHWALD, S. and SEXTON, B. A. (1977). *Appln. Surf. Sci.*, *1*, 1

IBACH, H. and ROWE, J. E. (1974a). *Surf. Sci.*, *43*, 481.

IBACH, H. and ROWE, J. E. (1974b). *Phys. Rev.*, *B9*, 1951.

IBACH, H. and ROWE, J. E. (1974c). *Phys. Rev.*, *B10*, 710.

IBACH, H. and SOMORJAI, G. A. (1979). *Appln. Surf. Sci.*, *3*, 293.

ITO, M. and SÜETAKA, W. (1977a). *Surf. Sci.*, *62*, 308.

ITO, M. and SÜETAKA, W. (1977b). *Proc. of 7th Int. Vac. Congr. and 3rd Int. Conf. on Solid Surfaces*, Vienna, p. 1043.

JAYASOORIYA, V. A., CHESTERS, M. A., HOWARD, M. W., KETTLE, S. F. A., POWELL, B. B. and SHEPPARD, N. (1980). *Surf. Sci.*, *93*, 526.

JENKINS, L. H. and CHUNG, M. F. (1971a). *Surf. Sci.*, *26*, 151.

JENKINS, L. H. and CHUNG, M. F. (1971b). *Surf. Sci.*, *28*, 409.

KAWAI, T., KUNIMORI, K., KONDOW, T., ONISHI, T. and TAMARU, K. (1974). *J. Chem. Soc. Faraday Trans. I*, *70*, 137.

KESMODEL, L. L., DUBOIS, L. H. and SOMORJAI, G. A. (1978). *Chem. Phys. Lett.*, *56*, 267.

KESSLER, J. and THIEME, F. (1977). *Surf. Sci.*, *67*, 405.

KRASSER, W., FADINI, A. and RENOUPREZ, A. (1980). *J. Mol. Struc.*, *60*, 427.

KUPPERMANN, A., FLICKER, W. N. and MOSHER, O. A. (1979). *Chem. Rev.*, *79*, 77.

KÜPPERS, J. (1972). *J. Electron Spectrosc. and Rel. Phenom.*, *1*, 186.

KÜPPERS, J. (1973). *Surf. Sci.*, *36*, 53.

LEGARE, P., HILAIRE, L., SOTTO, M. and MAIRE, G. (1980). *Surf. Sci.*, *91*, 175.

LEGARE, P., HOLL, Y. and MAIRE, G. (1979). *Solid State Commn.*, *31*, 307.

LEHWALD, S. and IBACH, H. (1979). *Surf. Sci.*, *89*, 425.

LEHWALD, S., IBACH, H. and DEMUTH, J. E. (1978). *Surf. Sci.*, *78*, 577.

LITTLE, L. H. (1966). In: *Infrared Spectra of Adsorbed Species*, Academic Press: New York.

LITTLE, L. H., SHEPPARD, N. and YATES, D. J. C. (1960). *Proc. Roy. Soc.* (*Lond.*), *A259*, 242.

LUDEKE, R. and KOMA, A. (1975). *Phys. Rev. Lett.*, *34*, 1170.

LUDEKE, R. and KOMA, A. (1976). *Phys. Rev.*, *B13*, 739.

LUSCHER, P. E. (1977). *Surf. Sci.*, *66*, 167.

LUSCHER, P. E. and PROPST, F. M. (1977). *J. Vac. Sci. and Tech.*, *14*, 400.

MAHAN, G. D. and LUCAS, A. A. (1978). *J. Chem. Phys.*, *68*, 1344.

MAIRE, G., LEGARE, P. and LINDAUER, G. (1979). *Surf. Sci.*, *80*, 238.

MCELHINEY, G., PAPP, H. and PRITCHARD, J. (1976). *Surf. Sci.*, *54*, 617.

MCELHINEY, G. and PRITCHARD, J. (1976). *Surf. Sci.*, *60*, 397.

MIYAMURA, M., SAKISAKA, Y., NISHIJIMA, M. and ONCHI, M. (1978). *Surf. Sci.*, *72*, 243.

MORROW, B. A. and SHEPPARD, N. (1969). *Proc. Roy. Soc.* (*Lond.*), *A311*, 391.

MURATA, Y., OHTANI, S. and TERADA, K. (1974). *Jap. J. Appl. Phys.* Suppl., *2* Part *2*, 837.

MUSKET, R. G. (1978). *Surf. Sci.*, *74*, 423.

NETZER, F. P., BERTEL, E. and MATTHEW, J. A. D. (1980). *Surf. Sci.*, *92*, 43.

NETZER, F. P. and MATTHEW, J. A. D. (1979a). *Surf. Sci.*, *81*, L 651.
NETZER, F. P. and MATTHEW, J. A. D. (1979b). *Solid State Commn.*, *29*, 209.
NETZER, F. P., WILLE, R. A. and MATTHEW, J. A. D. (1977). *Solid State Commn.*, *21*, 97.
NEWNS, D. M. (1977). *Phys. Lett.*, *60A*, 461.
NISHIJIMA, M. and FUJIWARA, K. (1977). *Solid State Commn.*, *24*, 101.
OHTANI, S., TERADA, K. and MURATA, Y. (1974). *Phys. Rev. Lett.*, *32*, 415.
PAPP, H. (1976). *Surf. Sci.*, *63*, 182.
PAPP, H. and PRITCHARD, J. (1975). *Surf. Sci.*, *53*, 371.
PAPAGEORGOPOULOUS, C. S. and DESPLAT, J. L. (1980). *Surf. Sci.*, *92*, 119.
PEARCE, H. A. and SHEPPARD, N. (1976). *Surf. Sci.*, *59*, 205.
PEARSON, B. N. J. (1980). *Surf. Sci.*, *92*, 265.
POWELL, R. A. (1979a). *Appln. Surf. Sci.*, *2*, 397.
POWELL, R. A. (1979b). *Appln. Surf. Sci.*, *2*, 439.
POWELL, C. J. and SWAN, J. B. (1960). *Phys. Rev.*, *118*, 640.
PRENTICE, J. D., LESIUNAS, A. and SHEPPARD, N. (1976). *J. Chem. Soc. Chem. Commn.*, 76.
RAO, C. N. R., SRINIVASAN, A. and JAGANNATHAN, K. (1981). *Indian J. Chem.* (in print).
RAO, C. N. R., SRINIVASAN, A., JAGANNATHAN, K. and HEGDE, M. S. (1980). *J. Sci. and Ind. Res.* (India), *39*, 212.
RAWLINGS, K. J., HOPKINS, B. J. and FOULIAS, S. D. (1978). *Surf. Sci.*, *77*, 561.
RICHARDSON, N. V. and BRADSHAW, A. M. (1979). *Surf. Sci.*, *88*, 255.
ROWE, J. E. and IBACH, H. (1973). *Phys. Rev. Lett.*, *31*, 102.
ROWE, J. E., IBACH, H. and FROITZHEIM, H. (1975). *Surf. Sci.*, *48*, 44.
RUBLOFF, G. W. and FREEOUF, J. L. (1978). *Phys. Rev.*, *B17*, 4680.
SAKISAKA, Y., AKIMOTO, K., NISHIJIMA, M. and ONCHI, M. (1979). *Solid State Commn.*, *29*, 121.
SAKISAKA, Y., MIYAMURA, M., TAMAKI, J., NISHIJIMA, M. and ONCHI, M. (1980). *Surf. Sci.*, *93*, 327.
SEXTON, B. A. (1979a). *Chem. Phys. Lett.*, *63*, 451.
SEXTON, B. A. (1979b). *Surf. Sci.*, *88*, 299.
SEXTON, B. A. (1979c). *Surf. Sci.*, *88*, 319.
SEXTON, B. A. (1980). *Surf. Sci.*, *94*, 435.
SHEPPARD, N. and NGUYEN, T. T. (1978). In: *Advances in Infrared and Raman Spectroscopy*, *5*, 67. (Ed. by R. J. H. Clark and R. E. Hester) Heyden: London.
SICKAFUS, E. N. and STEINRISSER, F. (1972). *Phys. Rev.*, *B6*, 3714.
SIMMONS, G. W. (1970). *J. Colloid and Interface Sci.*, *34*, 343.
SIMMONS, G. W. and SCHEIBNER, E. J. (1972). *J. Appl. Phys.*, *43*, 693.
SOMORJAI, G. A. (1979). *Surf. Sci.*, *89*, 496.
STEINRISSER, F. and SICKAFUS, E. N. (1971). *Phys. Rev. Lett.*, *27*, 992.
TAYLOR, T. N., ROGERS, J. W. and ELLIS, W. P. (1979). *J. Vac. Sci. and Tech.*, *16*, 581.
THIEL, P. A., WEINBERG, W. H. and YATES, JR., J. T. (1979a). *Chem. Phys. Lett.*, *67*, 403.
THIEL, P. A., WEINBERG, W. H. and YATES, JR., J. T. (1979b). *J. Chem. Phys.*, *71*, 1643.
THOMAS, G. E. and WEINBERG, W. H. (1978). *Phys. Rev. Lett.*, *41*, 1181.
THOMAS, G. E. and WEINBERG, W. H. (1979a). *J. Chem. Phys.*, *70*, 954.
THOMAS, G. E. and WEINBERG, W. H. (1979b). *J. Chem. Phys.*, *70*, 1000.
THOMAS, J. M. (1974). In: *Progress in Surface and Membrane Science*, *8*, 49. (Ed. by J. F. Danielli and D. A. Cadenhead). Academic Press: London and New York.
TRAJMAR, S., RICE, J. K. and KUPPERMANN, A. (1970). *Adv. Chem. Phys.*, *18*, 15.
UNERTL, W. N. and BLAKELY, J. M. (1977). *Surf. Sci.*, *69*, 23.
WENDELKEN, J. F. and ULEHLA, M. V. K. (1979). *J. Vac. Sci. and Tech.*, *16*, 441.
WILLE, R. A., NETZER, F. P. and MATTHEW, J. A. D. (1977). *Surf. Sci.*, *68*, 259.
WILLIS, R. F., (1979). *Surf. Sci.*, *89*, 457.
WILLIS, R. F., HO, W. and PLUMMER, E. W. (1979). *Surf. Sci.*, *80*, 593.
WILSON, J. M. (1976). *Surf. Sci.*, *57*, 499.